Do Monetary Policy Shocks Affect the Neutral Rate of Interest?

Danilo Leiva-León* Rodrigo Sekkel† Luis Uzeda‡

February 8, 2026

Abstract

We develop a Trend-Cycle Bayesian VAR that jointly estimates the real neutral rate of interest, r_t^*, and identifies monetary policy shocks. A key innovation is that the framework allows cyclical shocks, most notably monetary policy shocks, to affect the trend component of macroeconomic variables, providing a new way to assess whether transitory disturbances have persistent effects. Using external instruments, we find that contractionary monetary policy shocks reduce r_t^* and lower trend GDP growth, while the model's estimates of r_t^* remain consistent with standard benchmark measures. We then quantify the contribution of monetary policy shocks to the secular decline in r_t^*. Although these shocks at times generate sizable movements in r_t^*, their contribution to the long-run decline is modest, and their net effect on r_t^* since the early 1990s is slightly positive. We complement these findings with cross-country evidence from other advanced economies, pointing to similar effects.

JEL Classification: E32, E44, C32, C51

Keywords: Neutral rate of interest, monetary policy, trend-cycle BVAR.

We thank Jonas Arias, Gianluca Benigno, Fabio Canova, Efrem Castelnuovo, Marco del Negro, Martin Eichenbaum, Michael Ehrmann, Fillippo Ferroni, Jordi Gali, Marek Jarociński, Gary Koop, Matteo Luciani, Christian Matthes, Michele Lenza, Haroon Mumtaz, Evi Pappa, Benjamin Wong and seminar participants at the 2024 BSE Summer Forum, 2025 Society for Nonlinear Dynamics and Econometrics, 2025 RCEA Bayesian Econometrics Workshop, 2025 EABCN Conference: Advances in monetary policy and the natural rate of interest, Bank of Canada, CUNEF University, Universidad Carlos III, and the University of Strathclyde for their helpful comments and suggestions. The views expressed herein are solely those of the authors and should not be reported as representing the views of the Bank of Canada, the Federal Reserve Bank of Boston, the principals of the Board of Governors, or the Federal Reserve System. The authors declare that they have no conflict of interest and no relevant or material financial interests that relate to the research described in this paper.

*Federal Reserve Bank of Boston. E-mail: danilo.leiva-leon@bos.frb.org

†Bank of Canada. E-mail: rsekkel@bank-banque-canada.ca

‡Bank of Canada and CAMA. E-mail: luzedagarcia@bank-banque-canada.ca

1 Introduction

The real neutral rate of interest, r_t^*, has become a central input to monetary policy analysis and communication over the past two decades (Borio, 2021). Traditional frameworks view r_t^* as determined by slow-moving structural forces, such as technological change, demographics, inequality, and the convenience yield on safe assets (Laubach and Williams, 2003; Carvalho et al., 2016; Mian et al., 2021; Del Negro et al., 2017), and therefore largely insulated from monetary policy. This perspective reflects the common assumption that monetary policy has only transitory effects on economic activity and thus does not shift long-run saving and investment decisions.

Growing evidence challenges this view. Recent studies show that monetary policy can generate persistent effects on output and productivity, with implications for long-run growth and innovation (Moran and Queralto, 2018; Jordà et al., 2024; Elfsbacka-Schmöller et al., 2025). Other studies emphasize financial channels through which prolonged monetary easing may affect r_t^*, by shaping leverage cycles and crisis dynamics (Borio et al., 2019; Borio, 2021). Additionally, Rungcharoenkitkul and Winkler (2025) develop a New Keynesian model with mutual learning between central banks and private agents, in which r_t^* becomes endogenous to monetary policy shocks rather than purely determined by fundamentals. Taken together, these studies, whether directly or indirectly, question the long-standing assumption that r_t^* is exogenous to monetary policy.[1]

This paper contributes to this debate by developing a Trend-Cycle Bayesian Vector Autoregression (TC-BVAR) that jointly estimates r_t^*, and assesses whether monetary policy shocks affect its evolution. Estimating r_t^* and the policy shock within a unified framework circumvents the generated-regressors problem (Pagan, 1985; Heckman, 1986) that arises in two-step approaches that regress identified policy shocks on externally estimated measures of r_t^*. The framework also addresses the core identification challenge that r_t^* is latent and typically estimated with substantial uncertainty, while monetary policy both responds to and shapes key macroeconomic aggregates such as output and inflation. More broadly, our approach provides a general way to study whether cyclical disturbances—including monetary policy shocks—propagate into low-frequency movements in macroeconomic trends. In doing so, it allows us to assess the conventional orthogonality assumption between trend and cyclical dynamics and to shed light on the sources of trend-cycle interdependence.

Our key result shows that monetary policy shocks have a statistically significant and economically meaningful effect on the neutral rate: contractionary shocks—defined as unexpected increases in the short-term nominal interest rate—are associated with declines in r_t^*. This finding reinforces the recent view that monetary policy can shape macroeconomic outcomes beyond business-cycle frequencies, influencing the dynamics of r_t^*. Relatedly, it is well documented that r_t^* has followed a persistent downward trend since the early 1980s, with a pronounced decline during the global financial crisis of 2007-08 (see, e.g., Holston et al., 2017). Motivated by this stylized fact, our specification of r_t^*, in line with the Beveridge–Nelson decomposition (Beveridge and Nelson, 1981), models the neutral rate as a random walk driven by monetary policy shocks and other, non-identified distur-

[1] For a discussion of how r_t^* may also be influenced by non-structural factors—such as fiscal policy, the inflation target, and persistent supply shocks—see Nuño (2025).

bances. This formulation allows r_t^* to be expressed as the cumulative sum of these shocks over time, providing a natural framework to assess the extent to which monetary policy has influenced the historical trajectory of r_t^*.

Applying this framework, we find that while monetary policy shocks at times generate notable fluctuations in r_t^*—particularly during recessions such as 2001 and 2008-09—their contribution to its long-term downward trend is limited. Aggregated over the full sample, monetary policy shocks make a small but positive net contribution to r_t^*. This suggests (i) that monetary policy may have prevented r_t^* from declining further, and (ii) that the long-term decline in the neutral rate is unlikely to be driven by monetary policy itself, or by monetary policy *shocks* at the very least. The latter is consistent with broader evidence showing that monetary shocks typically account for only a modest share of the variation in key macroeconomic aggregates (Christiano et al., 1999; Smets and Wouters, 2007; Ramey, 2016). Importantly, our framework yields estimates of r_t^* that are broadly consistent with standard benchmarks such as Laubach and Williams (2003), Lubik and Matthes (2015), and Del Negro et al. (2017): prior to the global financial crisis, the neutral rate fluctuated between 2 and 2.5 percent, before declining toward 1 percent thereafter.

We also extend our baseline setup to shed light on the channels through which monetary policy may influence r_t^*. We proceed along two dimensions. First, given the theoretical link between r_t^* and long-run real economic growth, we augment our baseline TC-BVAR to include real GDP growth. The results suggest that contractionary monetary policy shocks lower trend GDP growth. This pattern is consistent with models featuring endogenous growth or hysteresis, as well as with empirical evidence documenting persistent effects of monetary policy on output, productivity and R&D investment (Moran and Queralto, 2018; Jordà et al., 2024; Elfsbacka-Schmöller et al., 2025).

Second, recognizing our measure of r_t^* may not fully purge a risk-premium component, we examine whether monetary policy shocks also affect the neutral rate through a term-premium channel. In contrast to the results for trend GDP growth, contractionary monetary policy shocks are found to have a small, positive, and statistically weak effect on the long-run term premium. This finding is in line with Hanson and Stein (2015), who document a positive relationship between monetary policy surprises and long-run real rates.[2] Taken together, these results suggest that the effect of monetary policy shocks on r_t^* is more likely to operate through real-economy channels than through financial-market channels.

Finally, we extend our analysis to other advanced economies: Canada, Japan, the United Kingdom, and the Euro area. Consistent with our results for the U.S., we find that contractionary (expansionary) monetary policy shocks lower (raise) r_t^*, although the magnitude of this effect varies somewhat across economies. The international evidence also indicates that monetary policy shocks play a limited role in shaping the long-run trajectory of r_t^*. These findings remain robust across alternative specifications, different external instruments, and sample periods.

[2]Specifically, Hanson and Stein (2015) show that an unexpected increase (decrease) in the short-term real rate leads to an increase (decrease) in long-run real rates, which they attribute to a term-premium effect arising from portfolio rebalancing by agents.

This paper relates to several strands of the literature. Methodologically, it connects to the extensive work on trend-cycle decompositions pioneered by Beveridge and Nelson (1981), Harvey (1985), Watson (1986), Clark (1987), and Morley et al. (2003), as well as to their multivariate extensions, including Evans and Reichlin (1994) and Morley et al. (2024). Our work is most closely related to the recent TC-BVAR models of Del Negro et al. (2017), Johannsen and Mertens (2021), Bianchi et al. (2023), and Fosso (2025). We extend this literature by allowing for trend-cycle correlation through the persistent effects of identified shocks in the cyclical block of the model. This approach differs from the orthogonal trend-cycle specifications in Del Negro et al. (2017), Johannsen and Mertens (2021), and Fosso (2025), and from Bianchi et al. (2023), who allow for trend-cycle correlation but model it using reduced-form shocks, which limits the economic interpretability of what underlies this type of correlation.

Our paper also contributes to the extensive literature on estimating r_t^*. In a seminal contribution, Laubach and Williams (2003) introduced a semi-structural model to jointly estimate r_t^* and potential output. Holston et al. (2017) extended this framework to a multi-country setting, confirming a broad decline in r_t^* post-financial crisis. Closer to our framework, Del Negro et al. (2017) employ a TC-BVAR similar to ours, while Lubik and Matthes (2015) estimate r_t^* using a time-varying parameter VAR with stochastic volatility. Our model produces estimates of r_t^* that are broadly consistent with these studies, while also enabling us to examine whether the neutral rate is affected by monetary policy shocks.

This paper is also related to the growing literature examining the long-run impact of monetary policy and other transitory demand shocks on the economy. Using an historical data set and the trilemma in international finance for identification, Jordà et al. (2024) estimate that monetary policy shocks affect the economy for over a decade. Importantly for the discussion around the determinants of the neutral rate, they find that measures of total factor productivity (TFP) exhibit strong hysteresis effects, consistent with the evidence in Ma and Zimmermann (2023) and Elfsbacka-Schmöller et al. (2025) on the effects of monetary policy on R&D investment. Antolin-Diaz and Surico (2022) and Cloyne et al. (2022) find persistent effects of transitory government spending and tax shocks, respectively. More broadly, Furlanetto et al. (2025) finds evidence of hysteresis, or permanent effects, of demand shocks.[3] We contribute to this literature by exploring the potential for monetary policy to exert hysteresis effects on the neutral rate of interest.

The remainder of the paper is organized as follows. Section 2 describes the econometric framework. Section 3 presents the main results. Section 4 discusses a set of robustness checks and extensions. Section 5 provides international evidence. Section 6 concludes.

[3]For a recent literature review on hysteresis and business cycles, see Cerra et al. (2023).

2 Methodology

This section describes the baseline model used to pursue three main objectives: (i) estimating r_t^*; (ii) identifying the monetary policy shock, e_t^{mp}; and (iii) linking e_t^{mp} to r_t^*. Each of these steps is part of a single unified estimation algorithm and discussed in turn. All main findings from the baseline specification also hold in the extensions examined in Section 4, which provide robustness checks.

2.1 Extracting r_t^* from a TC-BVAR

Our framework builds on common trend VAR models discussed in, for example, Del Negro et al. (2017), Johannsen and Mertens (2021) and Bianchi et al. (2023). In particular, we adopt a multivariate trend–cycle approach to describe a $N \times 1$ vector of observables, $\mathbf{y}_t$, with the following state-space representation:

$$\mathbf{y}_t = S\boldsymbol{\tau}_t + \mathbf{c}_t, \tag{1}$$

$$\mathbf{c}_t = \Phi_1 (\mathbf{y}_{t-1} - S\boldsymbol{\tau}_{t-1}) + \cdots + \Phi_p (\mathbf{y}_{t-p} - S\boldsymbol{\tau}_{t-p}) + \mathbf{u}_t, \tag{2}$$

$$\boldsymbol{\tau_t} = \boldsymbol{\tau_{t-1}} + \boldsymbol{\eta_t}, \tag{3}$$

$$\begin{bmatrix} \mathbf{u}_t \\ \boldsymbol{\eta_t} \end{bmatrix} \sim \mathcal{N}\left(\begin{bmatrix} \mathbf{0}_{N\times 1} \\ \mathbf{0}_{K\times 1} \end{bmatrix}, \begin{bmatrix} \boldsymbol{\Sigma}_u & \boldsymbol{\Sigma}_{u,\eta} \\ \boldsymbol{\Sigma}'_{u,\eta} & \boldsymbol{\Sigma}_\eta \end{bmatrix} \right). \tag{4}$$

Let S denote a reduced-rank $N \times K$ selection matrix that collects K common trends. Therefore, Equation (1) expresses the N variables in $\mathbf{y}_t$ as the sum of a low-frequency common-trend component, $S\boldsymbol{\tau}_t$, where $\boldsymbol{\tau}_t$ is a $K \times 1$ vector of common trends, and a cyclical component, $\mathbf{c}_t$, given by a $N \times 1$ vector. The latter is specified in (2) as a stationary VAR, where the roots of the lag polynomial $\Phi(L) = (I - \Phi_1 - \cdots - \Phi_p)$ lie outside the unit circle, such that each Φ_j for $j = 1, \cdots, p$ is a full $N \times N$ matrix. By contrast, the trend component $\boldsymbol{\tau}_t$ is modeled in (3) as a driftless random walk vector.

Equation (4) defines the variance–covariance matrix for the vector of innovations driving $\mathbf{c}_t$ and $\boldsymbol{\tau}_t$. A key difference from other recent applications of TC-BVARs (e.g., Del Negro et al. (2017), Johannsen and Mertens (2021), Ascari et al. (2023)) is that we allow for cross-covariance between $\mathbf{c}_t$ and $\boldsymbol{\tau}_t$. We discuss this in greater detail in Section 2.3, but it is sufficient to note here that in our setup such cross-covariance is a result of monetary policy shocks entering the law of motion for both $\mathbf{c}_t$ and $\boldsymbol{\tau}_t$.

Notably, the random-walk specification for modeling $\boldsymbol{\tau}_t$ is consistent with the Beveridge–Nelson (BN) decomposition (Beveridge and Nelson, 1981), which defines the trend of a time series as its long-horizon forecast. More formally,

$$\boldsymbol{\tau}_t = \lim_{h\to\infty} \mathbb{E}_t[\mathbf{y}_{t+h}].$$

In this sense, the BN decomposition is consistent with the common interpretation of r_t^* as a long-run

object, rather than a short-run cyclical one, and connects our framework with a number of studies that model low-frequency dynamics in a similar fashion.[4] In keeping with the BN decomposition, our estimation of r_t^* is based on the long-run Fisher equation relationship:

$$\lim_{h\to\infty} \mathbb{E}_t[i_{t+h}] = r_t^* + \pi_t^*, \tag{5}$$

which defines the expected long-run nominal interest rate, $\lim_{h\to\infty} \mathbb{E}_t[i_{t+h}]$, as the sum of two trends, r_t^* and trend inflation, π_t^*. In practice, to estimate these trends $\mathbf{y}_t$ should include both a measure of inflation and a measure of nominal interest rates. Accordingly, we specify:

$$\mathbf{y}_t = [\pi_t \ \pi_t^e \ i_t^{m_1} \ i_t^{m_2} \ i_t^{m_3}]',$$

where π_t denotes price inflation, π_t^e denotes inflation expectations, and $i_t^{m_j}$ for $j = 1, 2, 3$ are nominal interest rates at different maturities. Including multiple interest rates allows us to capture the connection between short- and long-term nominal rates and sharpens inference about r_t^*. It also helps address zero lower bound (ZLB) concerns, since longer-term rates were less constrained by the ZLB during the December 2008–December 2015 period. Incorporating measures of inflation expectations helps to better capture the long-run trend in inflation, which is key to estimating a long-run Fisher equation.[5]

Our baseline specification accommodates two latent trends, namely, π_t^*, and r_t^*, i.e., $\boldsymbol{\tau}_t = [\pi_t^* \ r_t^*]'$.[6] To identify these trends we make the following assumptions: the long-run Fisher equation relationship in (5) holds; π_t and π_t^e share a common trend (π_t^*); and r_t^* is a common trend among $i_t^{m_j}$ for $j = 1, 2, 3$. To parameterize these assumptions, we combine the selection matrix (S) with $\boldsymbol{\tau}_t$ as follows:[7]

$$S\boldsymbol{\tau}_t = \begin{bmatrix} 1 & 0 \\ 1 & 0 \\ 1 & 1 \\ 1 & 1 \\ 1 & 1 \end{bmatrix} \begin{bmatrix} \pi_t^* \\ r_t^* \end{bmatrix} = \begin{bmatrix} \pi_t^* \\ \pi_t^* \\ \pi_t^* + r_t^* \\ \pi_t^* + r_t^* \\ \pi_t^* + r_t^* \end{bmatrix}. \tag{6}$$

[4] See, e.g., Laubach and Williams (2003), Del Negro et al. (2017) and Morley et al. (2024) for other BN-based approaches to modeling r_t^*. See also Stock and Watson (2007) and Eo et al. (2023) for similar approaches applied to trend inflation.

[5] See Chan et al. (2018) for a related approach in which inflation expectations are used to sharpen inference on trend inflation.

[6] Section 3.4 explores alternative specifications whereby we allow for additional trends. Overall, our key results are virtually unchanged when introducing additional low-frequency components to our model.

[7] Following Del Negro et al. (2017), Johannsen and Mertens (2021), and Bianchi et al. (2023), we assume that the Fisher relation holds uniformly across nominal interest rates of different maturities. Likewise, the common trend in inflation is assumed to load equally on observed inflation and inflation expectations.

As a result, the measurement equation in (1) for our baseline specification can be cast as:

$$\mathbf{y}_t = \begin{bmatrix} \pi_t \\ \pi_t^e \\ i_t^{m_1} \\ i_t^{m_2} \\ i_t^{m_3} \end{bmatrix} = \begin{bmatrix} \pi_t^* \\ \pi_t^* \\ \pi_t^* + r_t^* \\ \pi_t^* + r_t^* \\ \pi_t^* + r_t^* \end{bmatrix} + \mathbf{c}_t, \tag{7}$$

where the last three equations make it clear that inference of a long-run Fisher equation, and consequently r_t^*, entails extracting signal from nominal interest rates at different maturities.

2.2 Identification of the Monetary Policy Shock

Beyond estimating r_t^*, our TC-BVAR framework must also identify the effects of monetary policy. To this end, we employ a Bayesian Proxy SVAR approach, following Caldara and Herbst (2019). Let z_t denote a scalar external proxy for a monetary policy shock, which is internalized in our system in (1) as follows:

$$\overbrace{\begin{bmatrix} \mathbf{y}_t \\ z_t \end{bmatrix}}^{\tilde{\mathbf{y}}_t} = \begin{bmatrix} S\boldsymbol{\tau}_t \\ 0 \end{bmatrix} + \begin{bmatrix} \Phi_1 & 0 \\ \mathbf{0}_{1\times N} & 0 \end{bmatrix} \begin{bmatrix} \mathbf{y}_{t-1} - S\boldsymbol{\tau}_{t-1} \\ 0 \end{bmatrix} + \cdots + \begin{bmatrix} \Phi_p & 0 \\ \mathbf{0}_{1\times N} & 0 \end{bmatrix} \begin{bmatrix} \mathbf{y}_{t-p} - S\boldsymbol{\tau}_{t-p} \\ 0 \end{bmatrix} + \overbrace{\begin{bmatrix} \mathbf{u}_t \\ v_t^z \end{bmatrix}}^{\tilde{\mathbf{u}}_t}. \tag{8}$$

The augmented vector of observables $\tilde{\mathbf{y}}_t$ uses z_t to provide additional information for identifying the monetary policy shock. Accordingly, the corresponding augmented vector of reduced-form errors $\tilde{\mathbf{u}}_t$ is decomposed as follows:

$$\overbrace{\begin{bmatrix} \mathbf{u}_t \\ v_t^z \end{bmatrix}}^{\tilde{\mathbf{u}}_t} = \overbrace{\begin{bmatrix} \Sigma_u^{tr} & 0 \\ \mathbf{a} & 1 \end{bmatrix}}^{A} \overbrace{\begin{bmatrix} \Omega_e^{1/2} & 0 \\ \mathbf{0}_{1\times N} & \sigma_v \end{bmatrix}}^{\Sigma_{\tilde{e}}^{1/2}} \overbrace{\begin{bmatrix} \mathbf{e}_t \\ v_t^{z*} \end{bmatrix}}^{\tilde{\mathbf{e}}_t}, \quad \begin{bmatrix} \mathbf{e}_t' & v_t^{z*} \end{bmatrix}' \sim \mathcal{N}(0,\ I_{N+1}), \tag{9}$$

where Σ_u^{tr} is a lower triangular matrix with ones on the main diagonal, and $\Omega_e^{1/2} = \texttt{diag}(\sigma_{e,1}, \cdots, \sigma_{e,N})$ is a diagonal matrix collecting the standard deviations of the orthogonalized shocks in $\mathbf{e}$. It follows that $\boldsymbol{\Sigma}_u = \Sigma_u^{tr}\Omega_e^{1/2}\Omega_e^{1/2}\Sigma_u^{tr\prime}$ in (4), and that $\tilde{\mathbf{u}}_t \sim \mathcal{N}\left(\mathbf{0}_{N+1\times 1},\ A\Sigma_{\tilde{e}}^{1/2}\Sigma_{\tilde{e}}^{1/2}A'\right)$ in (9), where A and $\Sigma_{\tilde{e}}^{1/2}$ denote, respectively, the impact matrix and the matrix of shock standard deviations for the proxy-augmented TC-BVAR.[8]

The key element for identification is the row vector $\mathbf{a}$. It is parameterized so that z_t provides information about the monetary policy shock but not about the other shocks in $\mathbf{e}$. Formally, we

[8] We assume homoskedastic reduced-form innovations. This assumption is motivated by two considerations. First, it avoids additional complexities that could introduce further uncertainty into the inference of monetary policy shocks. Second, the sample used in our baseline model excludes the two major episodes associated with changes in volatility–the pre-Great Moderation and post-Covid periods. This exclusion is not deliberate but reflects sample size constraints associated with the proxies used for z_t.

impose:

$$\mathbf{a} = (0,\ 0,\ \alpha_z,\ 0,\ 0,\ 0)\,, \tag{10}$$

$$\mathbf{e}_t = \left(e_t^{\pi},\ e_t^{\pi^e},\ e_t^{mp},\ e_t^{i_t^{m2}},\ e_t^{i_t^{m3}}\right)', \tag{11}$$

$$\mathbf{a}\mathbf{e}_t = \alpha_z e_t^{mp}. \tag{12}$$

From (11), we define the monetary policy shock as the third element of $\mathbf{e}_t$, as it corresponds to the short-term nominal interest rate ($i_t^{m_1}$) equation in the TC-BVAR in (7). Consequently, the identifying assumption is that e_t^{mp} is the only shock in the system that loads on both the proxy z_t and $i_t^{m_1}$.

Using the second row of (8) and (9), we can characterize the relationship between z_t and e_t^{mp} as:

$$z_t = \alpha_z e_t^{mp} + \sigma_v v_t^{z*}, \quad e_t^{mp} \perp v_t^{z*}. \tag{13}$$

This expression embeds the two standard assumptions underlying an instrumental-variable approach to shock identification: z_t is correlated with the shock of interest and orthogonal to all other shocks in $\mathbf{e}_t$. In particular, α_z governs the relevance of the instrument, since $\mathbb{C}\text{ov}(z_t, e_t^{mp}) = \alpha_z\, \mathbb{V}\text{ar}(e_t^{mp})$, which is nonzero whenever $\alpha_z \neq 0$. Moreover, the presence of measurement error v_t^{z*} helps mitigate attenuation bias, which could otherwise affect inference if z_t were used directly as a measure of the monetary policy shock.

2.3 Allowing for the Monetary Policy Shock to Impact r_t^*

The final element of our framework is to allow for the possibility that monetary policy shocks may affect r_t^*. With that in mind, we decompose the error term $\boldsymbol{\eta}_t$ in (3) as follows:

$$\boldsymbol{\eta}_t = H_\lambda \mathbf{e}_t + \boldsymbol{\eta}_t^*, \tag{14}$$

$$\begin{bmatrix} \mathbf{e}_t \\ \boldsymbol{\eta}_t^* \end{bmatrix} \sim \mathcal{N}\left(\begin{bmatrix} 0 \\ 0 \end{bmatrix},\ \begin{bmatrix} I_N & 0 \\ 0 & \boldsymbol{\Sigma}_{\eta^*} \end{bmatrix} \right), \tag{15}$$

where H_λ is a reduced rank $N \times K$ matrix that collects the impact of structural shocks in $\mathbf{e}_t$ on the common trends in $\boldsymbol{\tau}_t$. The second error term, $\boldsymbol{\eta}_t^*$, is a normally distributed vector that can be interpreted as collecting idiosyncratic shocks which, while not identified, allow for trend dynamics to be driven by other factors unrelated to monetary policy (or to any other factors driving short-run dynamics in $\mathbf{c}_t$). Given the representation of $\boldsymbol{\eta}_t$ in (14) and (15), the variance ($\boldsymbol{\Sigma}_\eta$) and covariance ($\boldsymbol{\Sigma}_{u,\eta}$) matrices in (4) take the following expressions:

$$\boldsymbol{\Sigma}_\eta = \boldsymbol{\Sigma}_{\eta^*} + H_\lambda H_\lambda', \tag{16}$$

$$\boldsymbol{\Sigma}_{\eta,u} = \mathbb{C}\text{ov}(H_\lambda \mathbf{e}_t,\ \Sigma_u^{tr} \Omega_e^{1/2} \mathbf{e}_t) = H_\lambda \Omega_e^{1/2} \Sigma_u^{tr\prime}. \tag{17}$$

For simplicity, we assume that $\mathbf{\Sigma}_{\eta^*}$ in (16) is diagonal. A comment is in order regarding the identification of $\mathbf{\Sigma}_{\eta,u}$ and $\mathbf{\Sigma}_{\eta^*}$. From equations (16) and (17), it is clear that estimation of these matrices relies on H_λ, that is, trend–cycle correlation, being identifiable. This observation connects our TC-BVAR approach with the class of correlated trend–cycle unobserved components (UC) models.[9] The conditions required for identification of correlation in this type of model are well established in both univariate (e.g., Morley et al. (2003) and Oh et al. (2008)) and multivariate UC settings (e.g., Trenkler and Weber (2016)). In short, akin to a method-of-moments approach, identification of H_λ depends on both order and rank conditions being satisfied when comparing the autocovariance function of our TC-BVAR with the autocovariance function implied by its VARIMA representation. In practice, this requires the order p of the lag polynomial $\Phi(L)$ for the VAR in (2) to be greater than or equal to two, a condition that is satisfied in our study, as we set $p = 4$.[10] From a Bayesian perspective, identification of trend-cycle correlation can also be assessed by comparing the posterior and prior distributions for the elements of H_λ. If the posterior distribution of an element differs substantially from its prior, this indicates that identification is driven by the data rather than by arbitrary prior choices. We revisit this issue when presenting results in Section 3.2.

Next, recall that in our baseline setup there are two long-run components given by π_t^* and r_t^*. Since our focus is on the effects of monetary policy shocks on r_t^*, we parameterize H_λ as follows:

$$H_\lambda = \begin{bmatrix} 0 & 0 & \lambda_\pi & 0 & 0 \\ 0 & 0 & \lambda_r & 0 & 0 \end{bmatrix}, \tag{18}$$

where the zero restrictions above ensure H_λ collects only the third element in the vector $\mathbf{e}_t$, i.e., the monetary policy shock e_t^{mp}.[11] Therefore, λ_π and λ_r capture the elasticity of π_t^* and r_t^* to e_t^{mp}, respectively. In this study, we are interested in λ_r, but report the results for λ_π in Appendix A.[12]

Combining (3), (14), and (18), we can write the law of motion for π_t^* and r_t^* as follows:

$$\pi_t^* = \pi_{t-1}^* + \lambda_\pi e_t^{mp} + \eta_t^{\pi^*}, \tag{19}$$

$$r_t^* = r_{t-1}^* + \lambda_r e_t^{mp} + \eta_t^{r^*}. \tag{20}$$

Naturally, estimates of λ_r are central to our analysis. From (20), if $\lambda_r = 0$, exogenous variation in monetary policy does not change r_t^*. Conversely, if $\lambda_r < 0$ ($\lambda_r > 0$), an unexpected increase in the policy rate r_t lowers (raises) r_t^*. Of course, the same rationale applies to λ_π in the context of π_t^*.

[9] Clearly, if $H_\lambda = 0$ there is no commonality between $\boldsymbol{\tau}_t$ and $\mathbf{c}_t$, and we have a standard orthogonal trend-cycle UC variant.

[10] In particular, since $\Phi(L)$ does not have a diagonal structure, Trenkler and Weber (2016) points out that to strengthen identification, for each dependent variable in the VAR the coefficients on its own lagged variable must be greater than the coefficients of lagged variables of other variables. This condition is induced by the high degree of cross-variable shrinkage in our prior for $\Phi(L)$.

[11] Also, as discussed in Section 4, we estimate an extension to our baseline model where the zero restrictions in (18) are relaxed, thereby allowing all orthogonalized shocks in $\mathbf{e}_t$ to affect π_t^* and r_t^*.

[12] While our framework is fairly general and can accommodate the effects of various identified shocks on multiple long-run trends, in this paper we focus specifically on the impact of monetary policy shocks on r_t^*. Examining the effects of these or other shocks on different trends is beyond the scope of this study and left for future research.

2.4 Estimation Procedure

Our framework consists of a state-space model estimated using Bayesian methods. In particular, we implement a Gibbs-sampling-based algorithm. This section provides a high-level overview of the estimation procedure, while a detailed description of the algorithm and the reparameterizations that enable a fully Gibbs-based estimation approach is relegated to the Supplementary Materials.

For convenience, we reproduce below the proxy-augmented measurement equation in (8):

$$\overbrace{\begin{bmatrix}\mathbf{y}_t\\ z_t\end{bmatrix}}^{\tilde{\mathbf{y}}_t} = \begin{bmatrix}S\boldsymbol{\tau}_t\\ 0\end{bmatrix} + \begin{bmatrix}\Phi_1 & 0\\ \mathbf{0}_{1\times N} & 0\end{bmatrix}\begin{bmatrix}\mathbf{y}_{t-1} - S\boldsymbol{\tau}_{t-1}\\ 0\end{bmatrix} + \cdots + \begin{bmatrix}\Phi_p & 0\\ \mathbf{0}_{1\times N} & 0\end{bmatrix}\begin{bmatrix}\mathbf{y}_{t-p} - S\boldsymbol{\tau}_{t-p}\\ 0\end{bmatrix} + \overbrace{\begin{bmatrix}\mathbf{u}_t\\ v_t^z\end{bmatrix}}^{\tilde{\mathbf{u}}_t}, \tag{21}$$

$$\tilde{\mathbf{u}}_t \sim \mathcal{N}\Big(\mathbf{0}_{N+1\times 1},\ A\Sigma_{\tilde{e}}^{1/2}\Sigma_{\tilde{e}}^{1/2}A'\Big), \tag{22}$$

where A and $\Sigma_{\tilde{e}}^{1/2}$ are defined in (9).

Inference based on the system above requires estimating $\boldsymbol{\tau}_t$ and three sets of parameters governing the cyclical component of the TC-BVAR: the autoregressive coefficients $(\Phi_1, \ldots, \Phi_p)$, the non-zero off-diagonal elements of the impact matrix A, and the variances along the main diagonal of $\Sigma_{\tilde{e}} = \Sigma_{\tilde{e}}^{1/2}\Sigma_{\tilde{e}}^{1/2}$. For notational convenience, we collect these parameters as follows. Let $\boldsymbol{\beta} = [\Phi_{1,1}, \ldots, \Phi_{1,p}, \ldots, \Phi_{N,1}, \ldots, \Phi_{N,p}]'$, where $\Phi_{i,j}$ denotes the i^{th} row of the j^{th} lag matrix Φ_j for $i = 1, \ldots, N$ and $j = 1, \ldots, p$. Let $\boldsymbol{\alpha} = [\boldsymbol{\alpha}_1, \ldots, \boldsymbol{\alpha}_N]'$, where $\boldsymbol{\alpha}_j$ collects all non-zero off-diagonal elements in the j^{th} row of A. Finally, let $\boldsymbol{\sigma}_{\tilde{e}}^2 = [\sigma_{e,1}^2,\ \cdots,\ \sigma_{e,N}^2,\ \sigma_v^2]$ collect the variances along the main diagonal of $\Sigma_{\tilde{e}}$.

Next, applying the change of variables $\eta_t^{k^*} = \sigma_{\xi,k^*}\xi_t^{k*}$ for $k \in \{\pi, r\}$, we rewrite the law of motion for the trends in (19) and (20) as:

$$\overbrace{\begin{bmatrix}\pi_t^*\\ r_t^*\end{bmatrix}}^{\boldsymbol{\tau}_t} = \begin{bmatrix}\pi_{t-1}^*\\ r_{t-1}^*\end{bmatrix} + \overbrace{\begin{bmatrix}\lambda_\pi\\ \lambda_r\end{bmatrix}}^{\boldsymbol{\lambda}} e_t^{mp} + \overbrace{\begin{bmatrix}\sigma_{\xi,\pi^*} & 0\\ 0 & \sigma_{\xi,r^*}\end{bmatrix}}^{\Sigma_{\xi^*}^{1/2}}\overbrace{\begin{bmatrix}\xi_t^{\pi*}\\ \xi_t^{r*}\end{bmatrix}}^{\boldsymbol{\xi}_t^*}, \quad \boldsymbol{\xi}_t^* \sim \mathcal{N}(\mathbf{0}_{2\times 1},\ I_2)\,. \tag{23}$$

This system introduces two additional sets of parameters: the vector of loadings $\boldsymbol{\lambda} = [\lambda_\pi, \lambda_r]'$ and $\boldsymbol{\sigma}_{\xi^*}^2 = [\sigma_{\xi,\pi^*}^2\ \sigma_{\xi,r^*}^2]$, which collects the variances of the non-monetary-policy-related shocks along the main diagonal of $\Sigma_{\eta^*} = \Sigma_{\xi^*}^{1/2}\Sigma_{\xi^*}^{1/2}$.

MCMC estimation of the state-space representation in (21)–(23) can thus be summarized as sequentially drawing from the following two conditional posterior distributions:

$$\begin{aligned}\texttt{(a) State-sampling step:}\quad & f(\boldsymbol{\tau} \mid \tilde{\mathbf{y}}, \boldsymbol{\theta}),\\ \texttt{(b) Parameter-sampling step:}\quad & f(\boldsymbol{\theta} \mid \tilde{\mathbf{y}}, \boldsymbol{\tau}),\end{aligned}$$

where $\tilde{\mathbf{y}} = [\tilde{\mathbf{y}}_1, \ldots, \tilde{\mathbf{y}}_T]'$, $\boldsymbol{\tau} = [\pi_1^*, r_1^*, \ldots, \pi_T^*, r_T^*]'$, and $\boldsymbol{\theta}$ denotes the collection of all parameters

appearing in (21)–(23). Specifically, $\boldsymbol{\theta} = \{\boldsymbol{\beta}, \boldsymbol{\alpha}, \boldsymbol{\sigma}^2_{\tilde{e}}, \boldsymbol{\sigma}^2_{\xi^*}, \boldsymbol{\lambda}\}$.

The conditional posterior for step (a) follows the approach in Leiva-León and Uzeda (2023) for correlated component time-varying parameter models, and constructs a likelihood function consistent with the trend–cycle correlation induced by the monetary policy shock affecting both $\boldsymbol{\tau}_t$ and the cyclical component $\mathbf{c}_t$. Since (21)–(23) define a Gaussian state-space system, the conditional posterior density of $\boldsymbol{\tau}$ is also Gaussian. For the parameters in $\boldsymbol{\theta}$, we adopt standard conjugate priors, which–combined with a Gaussian likelihood–yield closed-form conditional posteriors. Specifically, we use multivariate Gaussian priors for $\boldsymbol{\beta}$, $\boldsymbol{\alpha}$, and $\boldsymbol{\lambda}$, and inverse-gamma ($\mathcal{IG}$.) priors for each element of $\boldsymbol{\sigma}^2_{\tilde{e}}$ and $\boldsymbol{\sigma}^2_{\xi}$, which we denote by $\boldsymbol{\sigma}^2_{\tilde{e},i}$ and $\boldsymbol{\sigma}^2_{\xi,k}$, respectively. All priors are relatively uninformative, with the exception of the VAR coefficients in $\boldsymbol{\beta}$, for which we adopt a Minnesota-type prior, as is standard in VAR applications, to regularize coefficients on longer lags.[13]

Estimation proceeds by sequentially sampling from the following conditional posterior distributions:

$$(1)\ \boldsymbol{\tau} \mid \widetilde{\mathbf{y}},\ \boldsymbol{\theta} \sim \mathcal{N}\big(\overline{\mathbf{d}}_{\tau},\ \overline{\mathbf{D}}_{\tau}\big)\,,$$

$$(2)\ \boldsymbol{\beta} \mid \widetilde{\mathbf{y}},\ \boldsymbol{\tau},\ \boldsymbol{\theta}_{-\beta} \sim \mathcal{N}\big(\overline{\mathbf{d}}_{\beta},\ \overline{\mathbf{D}}_{\beta}\big)\,,$$

$$(3)\ \boldsymbol{\alpha}_i \mid \widetilde{\mathbf{y}},\ \boldsymbol{\tau},\ \boldsymbol{\theta}_{-\alpha_i} \sim \mathcal{N}\big(\overline{d}_{\alpha_i},\ \overline{D}_{\alpha_i}\big)\,, \qquad i = 2, \ldots, N+1,$$

$$(4)\ \boldsymbol{\sigma}^2_{\tilde{e},i} \mid \widetilde{\mathbf{y}},\ \boldsymbol{\tau},\ \boldsymbol{\theta}_{-\sigma^2_{\tilde{e},i}} \sim \mathcal{IG}.\big(\overline{v}_{\tilde{e},i},\ \overline{S}_{\tilde{e},i}\big)\,, \qquad i = 1, \ldots, N+1,$$

$$(5)\ \boldsymbol{\sigma}^2_{\xi^*,k} \mid \widetilde{\mathbf{y}},\ \boldsymbol{\tau},\ \boldsymbol{\theta}_{-\sigma^2_{\xi^*,k}} \sim \mathcal{IG}.\big(\overline{v}_{\xi^*,k},\ \overline{S}_{\xi^*,k}\big)\,, \qquad k \in \{\pi^*,\ r^*\},$$

$$(6)\ \boldsymbol{\lambda} \mid \widetilde{\mathbf{y}},\ \boldsymbol{\tau},\ \boldsymbol{\theta}_{-\lambda} \sim \mathcal{N}\big(\overline{\mathbf{d}}_{\lambda},\ \overline{\mathbf{D}}_{\lambda}\big)\,,$$

where $\boldsymbol{\theta}_{-\ell}$ denotes the parameter set $\boldsymbol{\theta}$ with element ℓ removed.

3 Main Results

This section evaluates how monetary policy shocks influence r_t^* using the framework outlined in Section 2. We begin by presenting our estimates of r_t^* and comparing them to benchmark estimates in the literature. We then quantify the elasticity of r_t^* with respect to monetary policy shocks. Next, we assess the contribution of monetary policy shocks to the observed evolution of the neutral rate. Finally, we extend the model to shed light on the mechanisms through which monetary policy transmits to r_t^*.

Our benchmark TC-BVAR model for the U.S. economy is estimated with data from 1989:Q1 through 2019:Q4.[14] It contains information on (i) price dynamics –CPI inflation and inflation expectations, (ii) interest rates – 3-Month U.S. Treasury Bill yield, 10-Year U.S. Treasury Note yield, and 20-Year U.S. Treasury Bond yield, and (iii) a series on exogenously defined monetary policy

[13] Following Giannone et al. (2015), the prior on $\boldsymbol{\beta}$ imposes an overall tightness parameter of 0.2. Moreover, the MCMC sampler retains only draws of $\boldsymbol{\beta}$ that lie inside the unit circle, ensuring a non-explosive cyclical component.

[14] The sample size is constrained by the availability of data for the monetary policy shock proxy.

surprises –proposed by Bauer and Swanson (2023)– that is used as instrument in the shock identification procedure. The motivation for employing these shocks in our baseline model specification is based on two key features. First, they are derived from a broader set of monetary policy announcement events, including press conferences, speeches, and testimonies by the Federal Reserve Chair, in addition to FOMC announcements. Second, they are computed by addressing the exogeneity issue, removing the component of monetary policy surprises that is correlated with economic and financial data. Further information about the observed variables included in the benchmark model is provided in Table A-1.

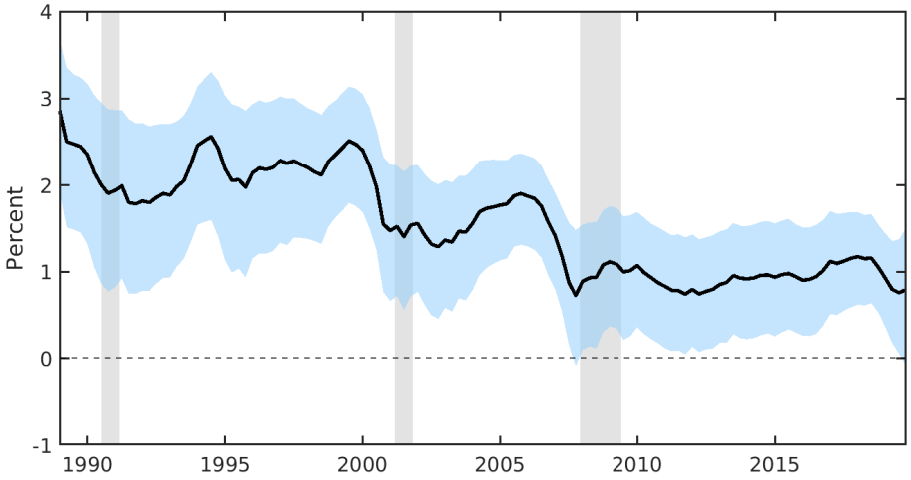
3.1 The Estimated Neutral Rate and Comparisons

The top panel of Figure 1 reports the estimate of r_t^* obtained from our baseline TC-BVAR. A salient feature of the series is its pronounced downward trend. As shown in the bottom panel of Figure 1, this pattern is closely aligned with alternative measures proposed in the literature, including Laubach and Williams (2003), Holston et al. (2017), Lubik and Matthes (2015), and Del Negro et al. (2017). In particular, r_t^* declines from around 3 percent in the early 1990s to roughly 1 percent by the end of the sample in 2019:Q4. Overall, our estimates exhibit similar levels and evolve in a comparable manner to these benchmarks. This consistency provides reassurance that the proposed framework yields a reliable measure of the neutral rate, which can be used to assess its relationship with monetary policy shocks.

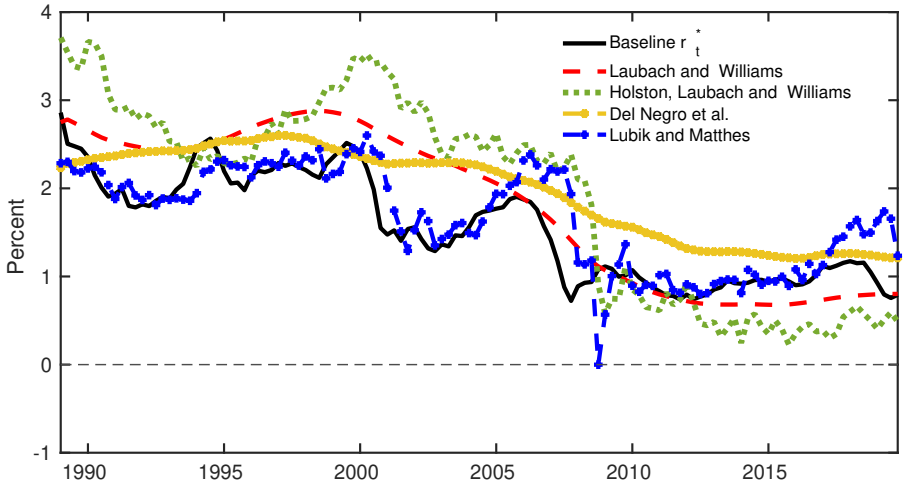
It is worth highlighting that these similarities arise despite the use of different modeling approaches. For example, Laubach and Williams (2003) and Holston et al. (2017) employ a state-space framework that lays out semi-structural relationships between output, inflation, and the interest rate, in which the natural rate of interest, r_t^*, is not directly identified from a Fisher relation but is instead inferred indirectly through its tight parametric link to additional latent states, such as potential output growth and other low-frequency components. In this class of models, r_t^* is therefore pinned down by the assumed dynamics of these underlying states rather than being directly disciplined by several observed interest rates. Moreover, in Laubach and Williams (2003) trend inflation is taken to be an exogenously defined observed variable rather than an estimated object. In principle, the choice of the variable used to measure trend inflation could have implications for the resulting estimates of r_t^*.

Instead, Lubik and Matthes (2015) rely on a time-varying parameter (TVP) VAR model to pin down underlying long-term trends, where the natural rate is inferred as the model's five-year-ahead forecast of the short-term real interest rate. In this case, no specific structural economic relations inform the model, and r_t^* reflects the persistent component of the forecasted real interest rate from the TVP-VAR. Del Negro et al. (2017), also employ a TC-BVAR model to estimate common trends associated with the interest rate and inflation and that are linked through the Fisher equation. However, their framework does not tackle the possible endogenous relation between the neutral rate and monetary policy, which is the focus of this paper.

FIGURE 1: Baseline and Comparative Estimates of r_t^*



A. Baseline r_t^*



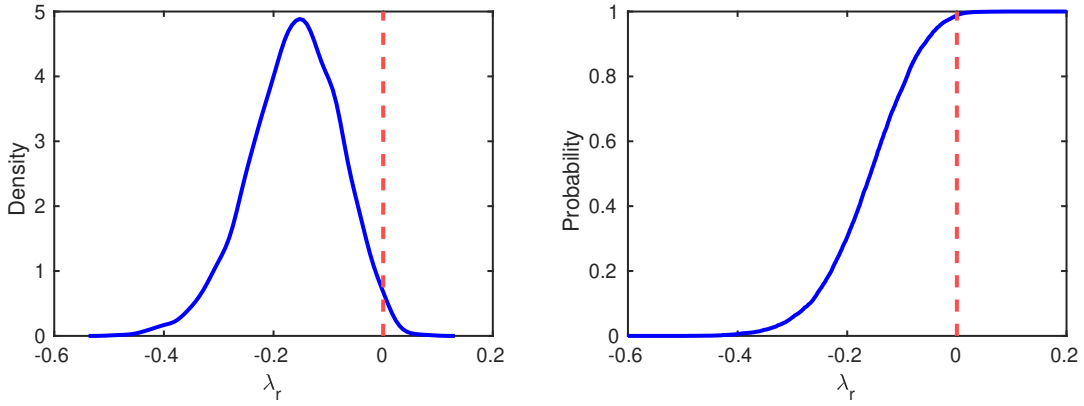
B. Selected alternative estimates of r_t^*

Note: The black line in the top panel plots the median of the posterior density of r_t^*. The light blue area shows the corresponding 90% credible set. The light gray vertical bars indicate recession periods as dated by the NBER. The sample period is 1988:Q1–2019:Q4. The bottom panel shows the baseline estimate of r_t^* from our TC-BVAR alongside alternative measures from the literature, namely: (i) the two-sided estimate of Laubach and Williams (2003); (ii) Holston et al. (2017); (iii) Del Negro et al. (2019); and (iv) Lubik and Matthes (2015).

3.2 The Elasticity of the Neutral Rate to Monetary Policy Shocks

As discussed in Section 2, our empirical framework allows us to jointly infer the neutral rate, monetary policy shocks, and the elasticity of the former to the latter (λ_r), as defined in Equation (20). Chart A of Figure 2 plots the posterior density of λ_r and shows that most of its mass lies at negative values and well separated from zero. Table A-2 reports a median estimate of -0.16, with the 10^{th} and 90^{th} percentiles equal to -0.27 and -0.10, respectively. These estimates imply

FIGURE 2: Elasticity of r_t^* to Monetary Policy Shocks



A. Posterior Density B. Cumulative Distribution Function

Note: Chart A shows the posterior density of the sensitivity (λ_r) of r_t^* to monetary policy shocks, as defined in Equation (20). Chart B shows the cumulative distribution function (CDF) of λ_r. In both charts, the vertical dashed red line denotes the prior mode of λ_r.

that a contractionary 25 basis point monetary policy shock lowers the neutral rate by about 4 basis points. Although this effect is modest in magnitude, it is precisely estimated and can translate into economically meaningful movements in r_t^* once its effects accumulate over time. We return to this issue in the next section.

Chart B of Figure 2 provides a complementary view of these results by reporting the cumulative distribution function of λ_r. It shows that the probability of a monetary policy shock having a positive effect on the neutral rate is only 0.01. Moreover, there is a 0.68 probability that a 25 basis point shock reduces the neutral rate by between 2 and 6 basis points. Together, the posterior density and its cumulative counterpart make clear that contractionary monetary policy shocks exert a statistically significant negative effect on the neutral rate of interest. Importantly, this result also speaks to identification, as discussed in Section 2.3. Since the prior for λ_r is centered at zero, the marked shift of posterior mass toward negative values indicates that the estimate is driven by the data rather than by prior information.

Overall, the results in Figure 2 align with a strand of the literature suggesting that monetary policy shocks can have persistent effects on the economy. For example, Jordà et al. (2024) exploit the trilemma of international finance to identify exogenous monetary policy changes in a panel of 17 advanced economies. They document effects that last for more than a decade, with particularly strong evidence of hysteresis in the capital stock and in total factor productivity–both traditionally viewed as key determinants of r_t^*. Similarly, a series of recent papers have examined the long-run impact of other transitory demand shocks, including Furlanetto et al. (2025) for aggregate demand shocks, Cloyne et al. (2022) for corporate tax shocks, and Antolin-Diaz and Surico (2022)

for government spending shocks.[15] These findings are also consistent with recent models, such as Stadler (1990) and Benigno and Fornaro (2018), which link aggregate demand, or monetary policy more broadly, to the growth rate of productivity. Furthermore, a supportive monetary policy environment may facilitate more efficient resource allocation among firms, thereby enhancing overall productivity and ultimately exerting upward pressure on the neutral rate (Baqaee et al. (2021); Gonzalez et al. (2023)). While these papers do not explicitly examine the link between exogenous monetary policy changes and r_t^*, they provide evidence that monetary policy–or, more generally, aggregate demand–affects the standard determinants of r_t^*.[16]

3.3 Monetary Policy and the Decline in the Neutral Rate

Next, we examine the importance of monetary policy shocks in explaining the estimated downward trend in r_t^*. To this end, recall that Equation (20) specifies r_t^* as a random walk. We can therefore re-express it as a function of the accumulated contributions of the two disturbances underlying r_t^*:

$$r_t^* = \underbrace{r_0^*}_{\text{Initial Condition}} + \underbrace{\lambda_r \sum_{\tau=1}^{t} e_\tau^{mp}}_{\text{Monetary Policy}} + \underbrace{\sum_{\tau=1}^{t} \eta_\tau^{r^*}}_{\text{Other Shocks}} . \tag{24}$$

Equation (24) is useful because it allows us to quantify the historical trajectory of r_t^* in terms of the cumulative effect of monetary policy shocks and the cumulative effect of other shocks. The latter category may encompass factors that shape long-term savings and investment decisions, such as technological advancements and demographic shifts. While our framework allows for the possibility that these factors influence r_t^*, it is not designed to identify them in detail. We therefore refer to them simply as 'other shocks' and focus on a decomposition that distinguishes between (i) innovations related to monetary policy, and (ii) those unrelated to monetary policy. The decomposition in Equation (24) also includes an initial condition term r_0^*, which is constant and thus does not affect the dynamic behavior of r_t^*.[17]

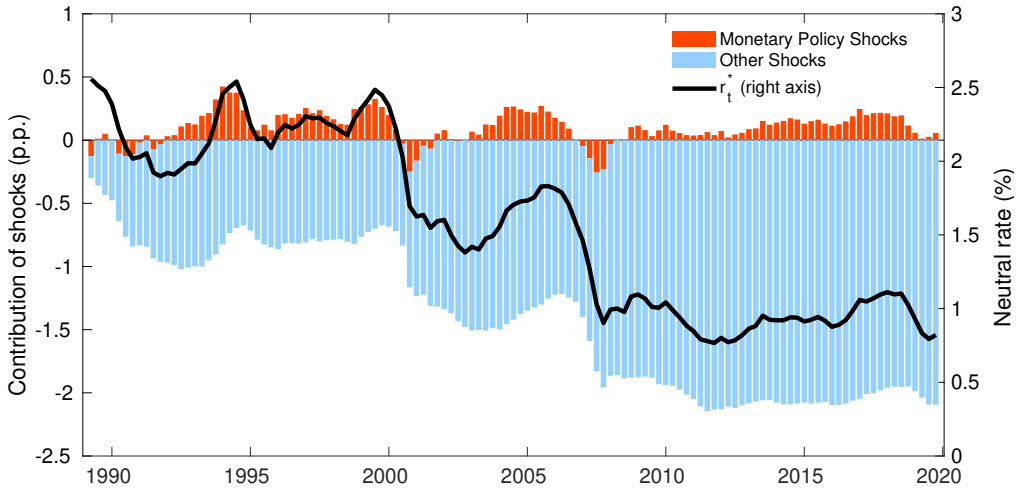
Figure 3 shows the contribution of monetary policy shocks ($\lambda_r \sum_{\tau=1}^{t} e_\tau^{mp}$) and other non-identified shocks ($\sum_{\tau=1}^{t} \eta_\tau^{r^*}$) to the long-term evolution of r_t^*. It is clear that monetary policy shocks do not explain a large fraction of r_t^* and are not responsible for its downward trend, as the model attributes most of the movements to other shocks. This interpretation aligns with the traditional view that the long-run behavior of r_t^* is ultimately governed by structural factors. Nevertheless, monetary policy shocks have at times played a role in explaining downturns in r_t^* around

[15] See Cerra et al. (2023) for a thorough recent discussion on the hysteresis evidence.

[16] We also examine the sensitivity of trend inflation to monetary policy shocks (λ_π). While the focus of the paper is on r_t^*, for completeness, we relegate results for trend inflation to the Appendix. The posterior distribution of λ_π, shown in Figure A-1 in Appendix A, is centered around zero, indicating that trend inflation does not respond contemporaneously to monetary policy shocks. This finding is consistent with Ascari and Fosso (2024), who argue that trend inflation is primarily driven by slow-moving structural forces–such as globalization, inflation expectations, technological change, and shifts in labor market conditions–rather than by short-run monetary policy disturbances.

[17] We treat r_0^* as the prior mean for τ_t at $t = 1$ in the state-sampling step of the MCMC algorithm described in Section 2.4. We set r_0 to the pre-sample three-decade average of the nominal short-term rate.

FIGURE 3: Cumulative Impact of Monetary Policy Shocks on r_t^*



Note: The colored bars plot the accumulated effect of monetary policy shocks ($\lambda_r \sum_{\tau=1}^{t} e_\tau^{mp}$) and other non-identified shocks ($\sum_{\tau=1}^{t} \eta_\tau^{r^*}$) on the evolution of the real neutral rate (r_t^*), aligned with the left axis. The black line plots the estimated r_t^*, aligned with the right axis. The difference between the estimated real neutral rate of interest and the sum of contributions corresponds to the initial condition (r_0^*), as defined in Equation (24). The sample period corresponds to 1988:Q1 – 2019:Q4.

recessions. For example, during the 2001 recession, monetary policy shocks account for roughly a quarter of the decrease in r_t^*. A similar contribution occurred during the global financial crisis of 2008-2009. Overall, our results show that monetary policy has had a net positive effect on the historical path of r_t^*, mitigating its decline. While the contributions from monetary policy shocks have fluctuated between about -0.5 and 0.5 percentage points, the contribution of other shocks has increased over time in relative terms, rising from 1 percentage point in the early 1990s to 2 percentage points in 2019.

Three comments are in order. First, it is arguably not surprising that monetary policy *shocks* do not account for the largest share of the variation in r_t^*. A large empirical literature finds that monetary policy shocks are not the dominant drivers of most macroeconomic indicators (Christiano et al., 1999; Smets and Wouters, 2007; Ramey, 2016).

Second, the contribution of monetary policy shocks to r_t^* naturally reflects their quantitative magnitude. Since the mid-1980s, monetary policy has operated under a more stabilizing regime, with substantially lower volatility in short-term nominal interest rates and, correspondingly, smaller policy surprises. In this context, the statistical significance of our estimate of λ_r is particularly informative: even relatively small and infrequent surprises leave a measurable imprint on r_t^*. This implies that a return to policy behavior associated with larger and more volatile interest rate movements, such as those observed in the 1970s, would likely strengthen the influence of monetary policy on r_t^*.

Third, our analysis follows the conventional approach of identifying monetary policy shocks

from unexpected movements in the short-term nominal interest rate. While the monetary policy toolkit has expanded since the global financial crisis to include instruments such as forward guidance and large-scale asset purchases, their relatively recent introduction and limited time-series availability would impose additional constraints on the feasible sample. We therefore abstract from unconventional monetary policy shocks but acknowledge the potential role that these additional monetary-policy-related sources may have on r_t^*, leaving their inclusion in our framework for future research.

3.4 An extended model with real GDP growth and term premium

After establishing a negative and statistically significant relationship between monetary policy shocks and r_t^*, we extend our TC-BVAR framework to shed light on the channels through which these shocks may operate. This extension is guided by two considerations. First, standard macroeconomic theory emphasizes a link between the neutral rate and long-run real economic growth, suggesting that persistent real effects of monetary policy may translate into movements in r_t^*. Second, empirical measures of r_t^* may not fully purge risk- or term-premium components, raising the possibility that monetary policy affects the neutral rate through financial-market channels rather than through fundamentals.

To evaluate the relative importance of these mechanisms, we augment the benchmark specification with year-over-year growth of quarterly real GDP (output growth hereafter).[18] This extension provides a parsimonious way to jointly infer: (i) a common trend between output growth and the three nominal interest rates (trend output growth hereafter) included in the baseline model; and (ii) a residual slow-moving component that captures low-frequency movements common to longer-maturity interest rates, beyond those accounted for by trend inflation and trend output growth, which, akin to Del Negro et al. (2017), we interpret as a trend in the term premium (trend term premium hereafter).[19] While the extension pursued in this section is not intended to provide a fully structural characterization of the transmission mechanism from monetary policy to the neutral rate, it provides informative evidence on the relative importance of competing channels.

More precisely, let g_t, g_t^*, and p_t^* denote the new elements included in this extended model, corresponding to observed output growth, trend output growth, and the trend term premium, respectively. While g_t is observed, g_t^* and p_t^* are latent components inferred from the model.

[18] Year-over-year real GDP growth is used to help isolate low-frequency movements in real activity; results are robust to using annualized quarterly real GDP growth instead. As part of a broader set of robustness checks, Section 4.3 extends the model to include multiple measures of real activity, each with its own (rather than a common) trend. Our key finding regarding the impact of monetary policy shocks on r_t^* remains unchanged.

[19] Residual low-frequency comovement across longer-maturity interest rates, after accounting for trend inflation and trend output growth, may reflect variation in compensation for interest rate risk or other risk-bearing considerations that affect long-term yields similarly across maturities.

Accordingly, we modify Equation 1 in the baseline TC-BVAR as follows:

$$\overbrace{\begin{bmatrix} \pi_t \\ \pi_t^e \\ g_t \\ r_t^{m_1} \\ r_t^{m_2} \\ r_t^{m_3} \end{bmatrix}}^{\mathbf{y}_t} = \overbrace{\begin{bmatrix} \pi_t^* \\ \pi_t^* \\ g_t^* \\ \pi_t^* + g_t^* \\ \pi_t^* + g_t^* + p_t^* \\ \pi_t^* + g_t^* + p_t^* \end{bmatrix}}^{S\boldsymbol{\tau}_t} + \mathbf{c}_t, \tag{25}$$

where $\mathbf{c}_t$ denotes the cyclical component, as defined in Equation (2).

As in the baseline specification, we allow these trends to respond endogenously to monetary policy shocks:

$$g_t^* = g_{t-1}^* + \lambda_g e_t^{mp} + \eta_t^{g^*}, \tag{26}$$

$$p_t^* = p_{t-1}^* + \lambda_p e_t^{mp} + \eta_t^{p^*}, \tag{27}$$

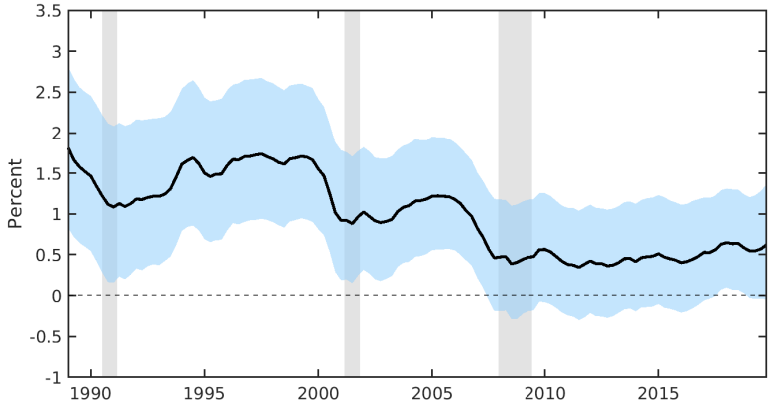
where the coefficients λ_g and λ_p capture the elasticity of trend output growth and the trend term premium to monetary policy shocks, respectively. The intuition behind (26)-(27) is simple. To the extent that the neutral rate depends on both g_t^* and p_t^*, these elasticities provide suggestive evidence on whether the response of r_t^* to monetary policy shocks reflects real-economy channels, financial-market channels, or both. All remaining elements of the model, including priors and the identification of monetary policy shocks, are unchanged relative to the benchmark specification described in Section 2.

Figure 4 shows the estimated latent trends g_t^* and p_t^*. In line with Laubach and Williams (2003) and Holston et al. (2017), trend output growth exhibits a high degree of comovement with the neutral rate estimates from the benchmark model (Figure 1), underscoring the relationship between long-run growth and r_t^*. By contrast, the term-premium trend follows a persistent downward trajectory, declining from around 2 percent in the early 1990s to roughly 0.5 percent by the end of the sample. These levels closely align with external estimates of the term premium on long-term Treasury securities obtained from the Federal Reserve Board's Three-Factor Nominal Term Structure Model.[20]

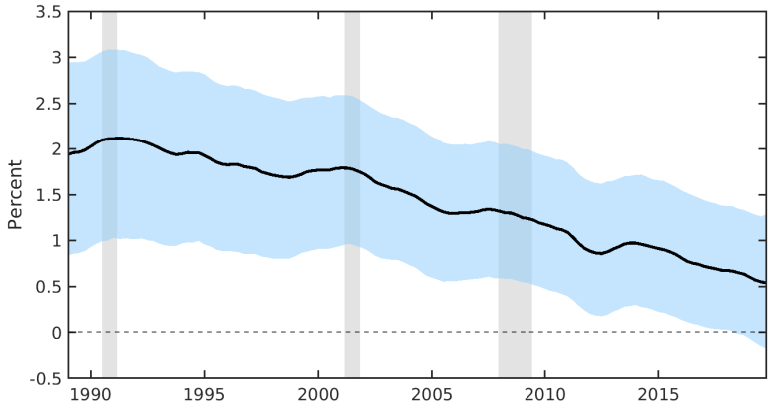
The posterior densities of the elasticities of trend output growth (λ_g) and the trend term premium (λ_p) with respect to monetary policy shocks are shown in Figure 5. We find clear evidence of a negative and statistically significant λ_g, with the posterior median close to -0.1, implying that a 100 basis point contractionary monetary policy shock reduces trend output growth by approximately 10 basis points. In contrast, the response of the term-premium trend is slightly positive but not statistically different from zero. Taking the mode of the posterior density for λ_p, its positive sign indicates that contractionary monetary policy shocks tend to raise the long-run term premium. This is consistent with the portfolio-rebalancing channel emphasized by Hanson and Stein (2015).

[20] See https://www.federalreserve.gov/data/three-factor-nominal-term-structure-model.htm.

FIGURE 4: Output Growth and Term Premium Trends



A. Output Growth (g_t^*)



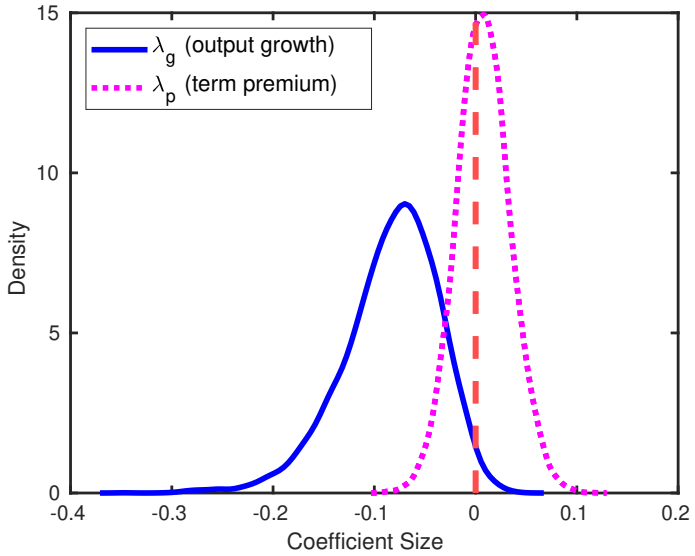
B. Term Premium (p_t^*)

Note: In each chart, the black line denotes the posterior median of the corresponding trend, and the light blue shaded area represents the 90% credible set. Light gray vertical bars indicate NBER recession periods. The sample period is 1988:Q1–2019:Q4.

Taken together, these findings suggest that the negative response of r_t^* to monetary policy shocks documented in the baseline model is more likely to reflect real-economy channels operating through long-run growth, rather than financial-market channels associated with term premia. This interpretation is consistent with models featuring endogenous growth or hysteresis, as well as with empirical evidence documenting persistent effects of monetary policy on output, productivity, and innovation (Moran and Queralto, 2018; Jordà et al., 2024; Elfsbacka-Schmöller et al., 2025).

It should be noted, however, that alternative mechanisms have been proposed in the literature that do not operate through fundamentals. For example, in Rungcharoenkitkul and Winkler (2025), within a New Keynesian incomplete-information framework, perceived movements in r_t^* can arise from a feedback loop between the central bank and the private sector: monetary policy actions shape private-sector beliefs about the neutral rate, and the private sector's responses in turn inform

FIGURE 5: Elasticities of Trend Growth and Trend Term Premium to Monetary Policy Shocks



Note: The figure reports the posterior densities of the sensitivities (λ_g and λ_p) of trend output growth and the trend term premium to monetary policy shocks, as defined in Equations (26) and (27), respectively. The vertical dashed red line denotes the prior mode of λ_g and λ_p.

the central bank's own beliefs. Notwithstanding differences in methodological approaches and transmission channels, both perspectives–our approach and that of the above-mentioned authors–point to the same implication: the neutral rate may respond endogenously to monetary policy actions.

4 Robustness

In this section, we conduct a series of robustness checks to validate our results. These exercises are designed to address three key aspects. (i) Alternative Instrumentation: we experiment with different monetary policy shocks to assess the sensitivity of our results to alternative choices of instruments. (ii) Multiple Shock Identification: we allow for the possibility that multiple shocks identified within the cyclical component of the model may influence the dynamics of the neutral rate. This ensures that our results are not driven by our choice to exclude other potential cyclical shocks that could affect r_t^* in our baseline model. (iii) Additional Controls: we incorporate additional control variables to allow for a richer information set and to reduce potential misspecification arising from a more parsimonious specification. This helps account for relevant lead–lag relationships that may be absent from the baseline model and provides a further check on the robustness of our results.

4.1 Using Different Instruments

As noted in Section 3, our baseline specification uses the monetary policy shocks of Bauer and Swanson (2023) as instruments in estimating the TC-BVAR model. To assess the robustness of the estimated elasticity of r_t^* to monetary policy shocks (λ_r in Equation 20), we re-estimate the

baseline TC-BVAR using four alternative measures of monetary policy shocks. In all cases, we keep the model specification and prior choices the same as in the baseline setup, varying only the time series used to instrument monetary policy shocks.

The four measures we use differ in their construction and underlying methodology. First, we employ the narrative monetary policy shocks proposed by Romer and Romer (2004). Second, we use the shocks proposed by Gertler and Karadi (2015), constructed from high-frequency surprises around policy announcements. Third, we consider the shocks proposed by Jarociński and Karadi (2020), which also use high-frequency surprises but account for the co-movement between interest rates and stock prices to isolate central bank information shocks. Finally, we employ the shocks proposed by Miranda-Agrippino and Ricco (2021), constructed by projecting market-based monetary surprises on their own lags and on the central bank's information set, as summarized by the Greenbook (now known as the Tealbook) forecasts, to control for information effects.

Because these measures are derived from different studies, their data coverage varies. As a result, the availability of data for each measure determines the sample used in each robustness check. Table A-1 provides a detailed description of the samples used in each exercise.

Figure 6 presents the posterior distribution of the elasticity of the neutral rate to monetary policy, λ_r, obtained using the four different monetary policy shocks as instruments in the identification strategy. Consistent with the estimates obtained with our benchmark specification, each alternative monetary policy instrument yields posterior distributions of λ_r that are concentrated on negative values. Table A-2 reports the median estimates along with the corresponding credible sets showing that point estimates range between -0.06 and -0.10 across the exercises, reinforcing the robustness of our baseline findings.

4.2 Allowing for Additional Shocks to Affect the Neutral Rate

In the baseline TC-BVAR, monetary policy shocks are the sole channel through which cyclical disturbances affect long-run trends through Equations (19) and (20). To allow for the possibility that other macroeconomic shocks also influence r_t^*, we assess the robustness of the estimated elasticity λ_r by relaxing the zero restrictions in H_λ in Equation (18), thereby permitting multiple cyclical shocks to affect long-run trends. As we do not seek a structural interpretation of these additional shocks, they correspond to the other components of the vector (11), along with e_t^{mp}, and are constructed by triangular factorization of $\mathbf{\Sigma}_u = \Sigma_u^{tr}\Omega_e^{1/2}\Omega_e^{1/2}\Sigma_u^{tr\prime}$.

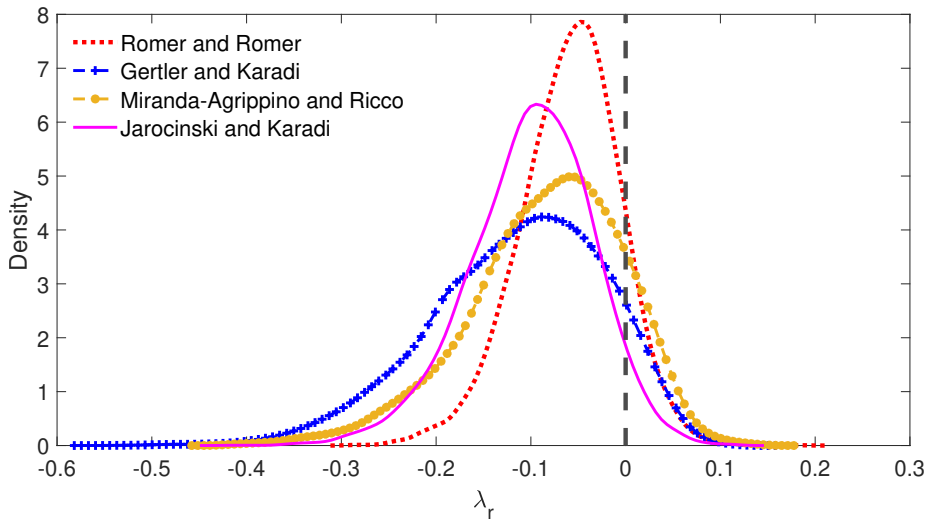
Under this specification, the law of motion for r_t^* in (20) becomes as follows:

$$r_t^* = r_{t-1}^* + \lambda_{r,1}e_t^{\pi} + \lambda_{r,2}e_t^{\pi^e} + \lambda_r e_t^{mp} + \lambda_{r,3}e_t^{i_t^{m2}} + \lambda_{r,4}e_t^{i_t^{m3}} + \eta_t^{r^*}, \tag{28}$$

where $\lambda_{r,i}$, for $i = 1, ..., 4$, measure the elasticity of r_t^* to all other shocks in the cyclical component of the model.[21] Both the priors and the identification of monetary policy shocks follow the baseline specification.

[21] We also allow these additional cyclical shocks to enter the law of motion for π_t^* in (19).

FIGURE 6: Posterior Density of λ_r Across Alternative Monetary Policy Shock Instruments



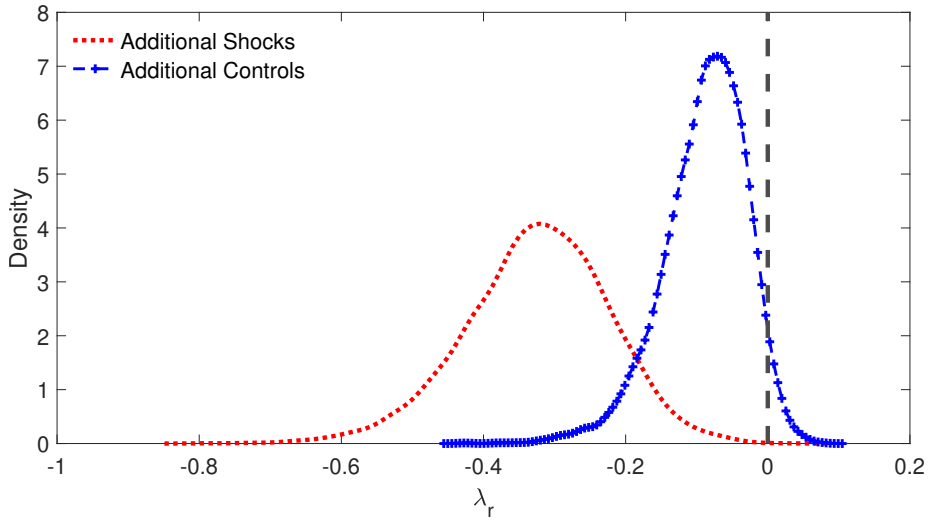
Note: The figure reports the posterior density of the sensitivity (λ_r) of r_t^* to monetary policy shocks, as defined in Equation (20), obtained using alternative instruments for monetary policy shocks: (i) Romer and Romer (2004) (red), (ii) Gertler and Karadi (2015) (blue), (iii) Miranda-Agrippino and Ricco (2021) (yellow), and (iv) Jarociński and Karadi (2020) (magenta). The vertical dashed black line denotes the prior mode of λ_r.

Figure 7 shows the posterior density of λ_r under this specification. The distribution shifts modestly toward more negative values, reinforcing that the estimated negative response of r_t^* to monetary policy shocks does not hinge on the baseline restriction that ties cyclical and trend components solely through these shocks. Figure A-3 in the Online Appendix reports the corresponding estimates of r_t^*. While allowing additional shocks to influence long-run trends naturally leads to somewhat greater variability in r_t^*, its overall dynamics remain close to those in the baseline. In sum, these results underscore the robustness of the negative effect of monetary policy shocks on r_t^* to alternative identifying assumptions.

4.3 Estimating a larger TC-BVAR model

The final robustness exercise expands the information set of the baseline model along two dimensions. First, we add real GDP growth and employment growth as additional indicators of real activity. Second, we incorporate a measure of financial conditions, the Excess Bond Premium of Gilchrist and Zakrajšek (2012), which captures variation in the price of bearing U.S. corporate credit risk beyond expected default compensation. The inclusion of financial conditions follows evidence that credit spreads and related measures play a central role in the transmission and propagation of monetary policy shocks (Caldara and Herbst, 2019; Miranda-Agrippino and Ricco, 2021). Table A-1 summarizes the data used in this extended specification. This exercise assesses the sensitivity of our benchmark estimates of the neutral rate and its elasticity to monetary policy shocks to the inclusion of these additional variables. Notably, we allow for a variable-specific trend for each of these additional controls. All other aspects of the specification, including prior calibration and the

FIGURE 7: Posterior Density of λ_r Across Alternative Model Specifications



Note: The figure reports the posterior density of the sensitivity (λ_r) of r_t^* to monetary policy shocks, as defined in Equation (20), associated with alternative model specifications. The vertical dashed black line denotes the prior mode of λ_r.

identification of monetary policy shocks, are kept identical to the baseline model.

Figure 7 reports the posterior density of the elasticity parameter under the extended specification. The posterior places most of its mass on negative values, with a median of -0.08 and 10th–90th percentile bounds of -0.16 and -0.02, respectively (Table A-2). These estimates are consistent with the baseline results, although the magnitude is somewhat smaller, and remain statistically different from zero. The corresponding estimates of r_t^*, shown in Figure A-4 in Appendix A, closely track those obtained under the benchmark specification.

The expanded information set also provides an additional check on the identification of monetary policy shocks. As shown by the impulse response functions in Figure A-5 in Appendix A, a contractionary monetary policy shock (i.e., an increase in the short-term nominal rate) raises the 3-Month U.S. Treasury Bill yield and leads to declines in real GDP, employment, and core inflation.[22] The impulse responses are constructed from the cyclical block of the model, which corresponds to a stationary VAR. These responses align with standard theoretical predictions and support the validity of the shock identification, while reinforcing the robustness of the results on the responsiveness of the neutral rate to monetary policy shocks.

5 International Evidence

Our previous results indicate that contractionary monetary policy shocks have a statistically significant negative effect on the U.S. neutral rate of interest. This section extends the analysis to other advanced economies: the U.K., the Euro area, Canada, and Japan. Together with the U.S.,

[22] We use core PCE inflation in this specification to mitigate price-puzzle concerns.

these economies constitute the full set of G7 countries. For each economy, we independently apply the model outlined in Section 2. Sample coverage varies across economies owing to differences in data availability. Macroeconomic data are obtained from the relevant national statistical agencies, and monetary policy shocks are drawn from publicly available estimates in the existing literature. Table A-1 in Appendix A provides detailed information on the sample periods, data sources, and monetary policy shock series utilized for each economic region.

5.1 International Neutral Rates

Figure 8 reports our estimates of r_t^* for the four economies considered. Consistent with the existing literature, including Holston et al. (2017) and subsequent contributions by Del Negro et al. (2019), Glick (2020), and Ferreira and Shousha (2023), the estimates display a sustained decline in r_t^* over the sample period. This decline is common across economies and becomes particularly pronounced around the 2008-09 global financial crisis.

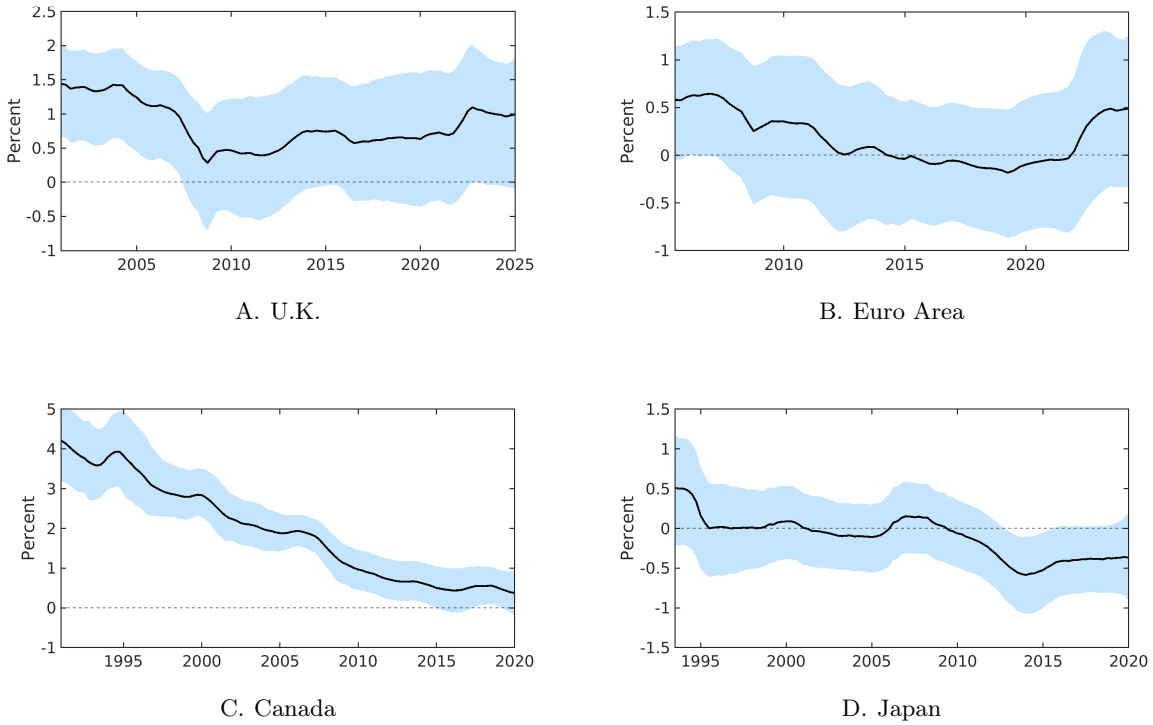
We also estimate an increase in r_t^* following the onset of the COVID-19 pandemic in both the U.K. and the euro area. The increase is relatively modest in the U.K., whereas in the euro area r_t^* rises more markedly and remains elevated from 2021 onward. This pattern is consistent with recent euro-area estimates reported by the ECB in Brand et al. (2024) and Brand et al. (2025).

Our estimates of the neutral rate for the U.K. and Canada are also closely aligned with those reported by Lubik et al. (2024), both in levels and dynamics. This alignment is notable given that Lubik et al. (2024) employ a country-specific TVP-VAR, providing an independent benchmark based on a distinct modeling approach. For Japan, our estimates closely track both the level and evolution of the neutral rate reported by Fujiwara et al. (2016), who use a natural yield curve framework that exploits information across multiple maturities.

5.2 Monetary Policy Shocks and International Neutral Rates

We next examine the estimated elasticity of r_t^* with respect to monetary policy shocks across these economies. Figure 9 reports the posterior distributions of the coefficient λ_r in Equation (20), which governs this elasticity for each country. In line with our U.S. results, the posterior modes are negative in all four economies, with some cross-country heterogeneity in magnitude, implying that contractionary monetary policy shocks are associated with declines in r_t^* across all economies considered. Appendix Table A-2 reports the median estimates of λ_r together with the 10th and 90th percentile credible intervals, providing a summary of the estimated magnitude and uncertainty.

FIGURE 8: Neutral Rates Across Selected Economies



A. U.K. B. Euro Area

C. Canada D. Japan

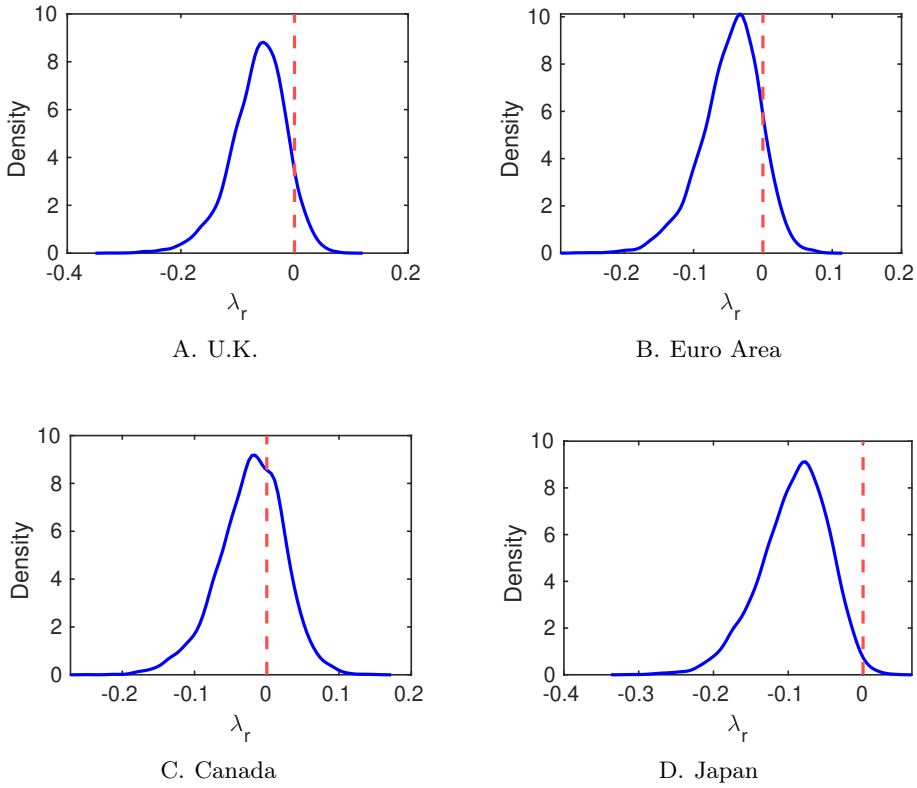
Note: The figure plots the median of the posterior density of r_t^* for four countries: (a) the U.K., (b) Euro Area, (c) Canada, and (d) Japan. The light blue area shows the corresponding 90% credible sets. The sample period varies by country. See Table A-1 for details.

When looking at the median point estimates, we observe some heterogeneity in the elasticity of neutral rates to monetary policy shocks across advanced economies. While the U.S. exhibits a relatively strong elasticity of -0.16 in our baseline specification, other advanced economies display more modest responses, with elasticities ranging between -0.09 and -0.02. The statistical significance of these estimates also varies considerably across countries. Evidence varies across economies. The United Kingdom and Japan display the strongest relationship, with posterior densities centered further from zero; Japan exhibits the largest estimated elasticity, around -0.1. In contrast, Canada shows the weakest evidence, with wide credible intervals that include values near zero, indicating greater uncertainty. The euro area lies between these cases, with moderate evidence of an effect that is smaller than in the United States, Japan, or the United Kingdom.

5.3 Decomposing International Neutral Rates

We next examine the contribution of monetary policy shocks to the secular decline in r_t^* across these economies. Using the decomposition in Equation (24), we separate movements in the neutral rate into components attributable to monetary policy shocks and to other factors. Figure 10 shows the historical decomposition of neutral rates across these G7 economies, revealing some heterogeneity

FIGURE 9: Elasticity of r_t^* to Monetary Policy Shocks Across Selected Economies



A. U.K. B. Euro Area

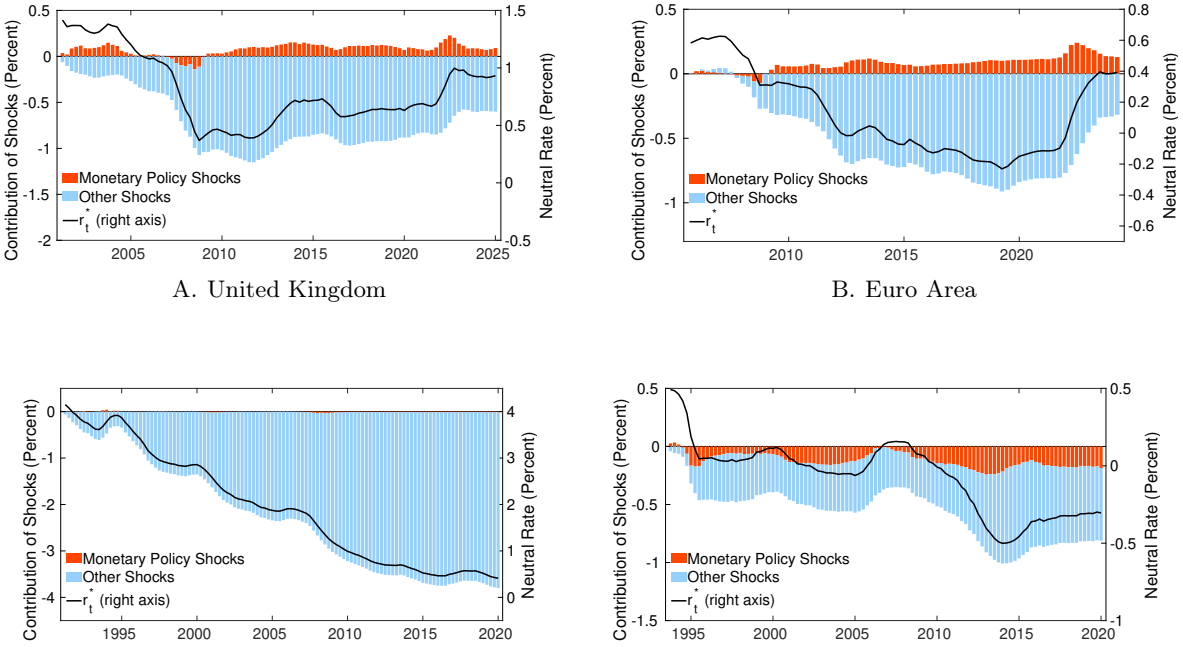
C. Canada D. Japan

Note: The figure reports the posterior density of the sensitivity (λ_r) of r_t^* to monetary policy shocks, as defined in Equation (20). The vertical dashed red line denotes the prior mode of λ_r.

in how monetary policy shocks have shaped r_t^* over time.

The contribution of monetary policy shocks to movements in r_t^* differs across economies, consistent with the heterogeneity documented in earlier sections. In the U.K. and the euro area, monetary policy shocks have generally contributed to increases in r_t^* over the sample period, mirroring the U.S. results, with particularly pronounced positive contributions in 2022 amid the policy response to elevated inflation. Japan exhibits a contrasting pattern, with monetary policy shocks exerting persistent downward pressure on r_t^*, consistent with its prolonged period where monetary policy was constrained by the zero lower bound. In Canada, by contrast, monetary policy shocks do not display a statistically meaningful contribution to r_t^* dynamics, suggesting a more limited role for monetary policy relative to other determinants over the sample period.

FIGURE 10: Cumulative Impact of Monetary Policy Shocks on r_t^* Across Selected Economies



A. United Kingdom

B. Euro Area

C. Canada

D. Japan

Note: The colored bars plot the accumulated effect of monetary policy shocks ($\lambda_r \sum_{\tau=1}^{t} e_\tau^{mp}$) and other non-identified shocks ($\sum_{\tau=1}^{t} \eta_\tau^{r^*}$) on the evolution of the real neutral rate (r_t^*) for each country, aligned with the left axis. The black line plots the estimated r_t^*, aligned with the right axis. The difference between the estimated neutral rate and the sum of contributions corresponds to the initial condition (r_0^*), as defined in Equation (24). The sample period varies by country. See Table A-1 for details.

6 Conclusion

This paper proposes a Trend-Cycle Bayesian VAR framework that jointly estimates the neutral rate and assesses the extent to which monetary policy influences its long-run evolution. The framework allows identified monetary policy shocks originating in the cyclical block to enter directly into the law of motion of the neutral rate, thereby relaxing the conventional orthogonality assumptions that treat r_t^* as insulated from policy actions. Despite this added flexibility, the resulting estimates of r_t^* remain closely aligned with standard benchmark measures in the literature. At the same time, the framework provides a systematic way to evaluate how cyclical disturbances, and monetary policy in particular, can shape the dynamics of macroeconomic trends such as the neutral rate.

Our key result indicates that contractionary monetary policy shocks have a statistically significant and economically meaningful negative effect on the neutral rate, providing support for models featuring endogenous growth or hysteresis (Benigno and Fornaro, 2018; Moran and Queralto, 2018) as well as with empirical evidence documenting persistent effects of monetary policy on output, productivity and R&D investment (Ma and Zimmermann, 2023; Jordà et al., 2024; Elfsbacka-Schmöller et al., 2025). However, while these shocks generate sizable fluctuations in the

neutral rate at business-cycle frequencies, particularly around major recessions, their contribution to the secular decline in the neutral rate since the early 1990s is limited. If anything, the cumulative effect of monetary policy shocks over the sample is slightly positive, suggesting that monetary policy has tended to mitigate, rather than amplify, the long-run downward drift in the neutral rate. Extensions of the framework point to real-economy channels, operating through persistent effects on trend output growth, as the primary mechanism linking monetary policy shocks to the neutral rate, with little evidence that term-premium channels play a central role.

Overall, these findings help reconcile two views that are often seen as competing. On the one hand, they support the conventional perspective that long-run movements in the neutral rate are primarily driven by slow-moving structural forces that lie largely outside the direct control of monetary policy. On the other hand, they indicate that monetary policy does influence the evolution of the neutral rate, even if its long-run quantitative contribution is modest. In environments characterized by less systematic and more volatile monetary policy, such as those observed in the 1970s, monetary policy shocks could therefore exert a more sizable cumulative influence on the neutral rate. More broadly, the framework introduced in this paper provides a general approach for studying how cyclical shocks can propagate into trend dynamics. Extending this framework to other shocks and trend components is a natural avenue for future research.

References

Antolin-Diaz, J. and P. Surico (2022): *The long-run effects of government spending*, Centre for Economic Policy Research.

Ascari, G., P. Bonomolo, and Q. Haque (2023): "The Long-Run Phillips Curve is a Curve," CAMA Working Paper 37/2023, Centre for Applied Macroeconomic Analysis, Crawford School of Public Policy, The Australian National University.

Ascari, G. and L. Fosso (2024): "The international dimension of trend inflation," *Journal of International Economics*, 148, 103896.

Baqaee, D., E. Farhi, and K. Sangani (2021): "The supply-side effects of monetary policy," NBER Working Paper 28345, National Bureau of Economic Research.

Bauer, M. D. and E. T. Swanson (2023): "A reassessment of monetary policy surprises and high-frequency identification," *NBER Macroeconomics Annual*, 37, 87–155.

Benigno, G. and L. Fornaro (2018): "Stagnation traps," *The Review of Economic Studies*, 85, 1425–1470.

Beveridge, S. and C. R. Nelson (1981): "A New Approach to the Decomposition of Economic Time Series into Permanent and Transitory Components with Particular Attention to the Measurement of the 'Business Cycle'," *Journal of Monetary Economics*, 7, 151–174.

Bianchi, F., G. Nicolò, and D. Song (2023): "Inflation and real activity over the business cycle," Tech. rep., National Bureau of Economic Research.

Borio, C. (2021): "Navigating by r*: safe or hazardous?" Tech. rep., Bank for International Settlements.

Borio, C. E., P. Disyatat, and P. Rungcharoenkitkul (2019): "What anchors for the natural rate of interest?" .

Brand, C., N. Lisack, and F. Mazeliz (2024): "Estimates of the natural interest rate for the euro area: an update," ECB Economic Bulletin 2024-1, European Central Bank.

——— (2025): "Natural rate estimates for the euro area: insights, uncertainties and shortcomings," ECB Economic Bulletin 2025-1, European Central Bank.

Braun, R., S. Miranda-Agrippino, and T. Saha (2025): "Measuring monetary policy in the UK: The UK monetary policy event-study database," *Journal of Monetary Economics*, 149, 103645.

Caldara, D. and E. Herbst (2019): "Monetary policy, real activity, and credit spreads: Evidence from Bayesian proxy SVARs," *American Economic Journal: Macroeconomics*, 11, 157–192.

Carvalho, C., A. Ferrero, and F. Nechio (2016): "Demographics and real interest rates: Inspecting the mechanism," *European Economic Review*, 88, 208–226.

Cerra, V., A. Fatás, and S. C. Saxena (2023): "Hysteresis and business cycles," *Journal of Economic Literature*, 61, 181–225.

Champagne, J. and R. Sekkel (2018): "Changes in monetary regimes and the identification of monetary policy shocks: Narrative evidence from Canada," *Journal of Monetary Economics*, 99, 72–87.

Chan, J. C., T. E. Clark, and G. Koop (2018): "A new model of inflation, trend inflation, and long-run inflation expectations," *Journal of Money, Credit and Banking*, 50, 5–53.

Chan, J. C. and I. Jeliazkov (2009): "MCMC Estimation of Restricted Covariance Matrices," *Journal of Computational and Graphical Statistics*, 18, 457–480.

Christiano, L. J., M. Eichenbaum, and C. L. Evans (1999): "Monetary policy shocks: What have we learned and to what end?" *Handbook of macroeconomics*, 1, 65–148.

Clark, P. K. (1987): "The Cyclical Component of U. S. Economic Activity," *Quarterly Journal of Economics*, 102, 797–814.

Cloyne, J., J. Martinez, H. Mumtaz, and P. Surico (2022): "Short-term tax cuts, long-term stimulus," Tech. rep., National Bureau of Economic Research.

Del Negro, M., D. Giannone, M. P. Giannoni, and A. Tambalotti (2017): "Safety, liquidity, and the natural rate of interest," *Brookings Papers on Economic Activity*, 2017, 235–316.

——— (2019): "Global trends in interest rates," *Journal of International Economics*, 118, 248–262.

Elfsbacka-Schmöller, M., O. Goldfayn-Frank, and T. Schmidt (2025): "Beyond the Short Run: Monetary Policy and Innovation Investment," *Discussion Paper Deutsche Bundesbank 18/2025*.

Eo, Y., L. Uzeda, and B. Wong (2023): "Understanding trend inflation through the lens of the goods and services sectors," *Journal of Applied Econometrics*, 38, 751–766.

Evans, G. and L. Reichlin (1994): "Information, forecasts, and measurement of the business cycle," *Journal of monetary economics*, 33, 233–254.

Ferreira, T. and S. Shousha (2023): "Determinants of global neutral interest rates," *Journal of International Economics*, 145, 103833.

Fosso, L. (2025): "Decomposing US economic fluctuations: a trend-cycle approach," Working Paper Series 3138, European Central Bank, Frankfurt am Main, Germany, european Central Bank Working Paper Series No. 3138.

Fujiwara, S., Y. Iwasaki, I. Muto, K. Nishizaki, and N. Sudo (2016): "Developments in the natural rate of interest in Japan," Review Series 16-E-12, Bank of Japan.

Furlanetto, F., A. Lepetit, Ø. Robstad, J. Rubio-Ramírez, and P. Ulvedal (2025): "Estimating hysteresis effects," *American Economic Journal: Macroeconomics*, 17, 35–70.

Gertler, M. and P. Karadi (2015): "Monetary policy surprises, credit costs, and economic activity," *American Economic Journal: Macroeconomics*, 7, 44–76.

Giannone, D., M. Lenza, and G. E. Primiceri (2015): "Prior Selection for Vector Autoregressions," *Review of Economics and Statistics*, 97, 436–451.

Gilchrist, S. and E. Zakrajšek (2012): "Credit Spreads and Business Cycle Fluctuations," *American Economic Review*, 102, 1692–1720.

Glick, R. (2020): "R* and the Global Economy," *Journal of International Money and Finance*, 102, 102105.

Gonzalez, B., G. Nuño, D. Thaler, and S. Albrizio (2023): "Firm heterogeneity, capital misallocation and optimal monetary policy," BIS Working Papers 1148, Bank for Intrenational Settlements.

Hanson, S. G. and J. C. Stein (2015): "Monetary policy and long-term real rates," *Journal of Financial Economics*, 115, 429–448.

Harvey, A. C. (1985): "Trends and cycles in macroeconomic time series," *Journal of Business & Economic Statistics*, 3, 216–227.

Heckman, J. J. (1986): "An Alternative Evaluation of Traditional Estimators of the Household Production Function," *Econometrica*, 54, 1269–1296.

Holston, K., T. Laubach, and J. C. Williams (2017): "Measuring the natural rate of interest: International trends and determinants," *Journal of International Economics*, 108, S59–S75.

Jarociński, M. and P. Karadi (2020): "Deconstructing monetary policy surprises – the role of information shocks," *American Economic Journal: Macroeconomics*, 12, 1–43.

Johannsen, B. K. and E. Mertens (2021): "A Time-Series Model of Interest Rates with the Effective Lower Bound," *Journal of Money, Credit and banking*, 53, 1005–1046.

Jordà, Ò., S. R. Singh, and A. M. Taylor (2024): "The long-run effects of monetary policy," *Review of Economics and Statistics*, Forthcoming.

Kroese, D. P. and J. C. Chan (2014): *Statistical Modeling and Computation*, New York, NY, USA: Springer, 1st ed.

Kubota, H. and M. Shintani (2022): "High-frequency identification of monetary policy shocks in Japan," *The Japanese Economic Review*, 73, 483–513.

Laubach, T. and J. C. Williams (2003): "Measuring the natural rate of interest," *Review of Economics and Statistics*, 85, 1063–1070.

Leiva-León, D. and L. Uzeda (2023): "Endogenous time variation in vector autoregressions," *Review of Economics and Statistics*, 105, 125–142.

Lubik, T., B. Merone, and N. Robino (2024): "Stargazing: Estimating r* in Other Countries," Economic Brief 24-10, Federal Reserve Bank of Richmond.

Lubik, T. A. and C. Matthes (2015): "Calculating the natural rate of interest: A comparison of two alternative approaches," *Richmond Fed Economic Brief*.

Ma, Y. and K. Zimmermann (2023): "Monetary policy and innovation," Tech. rep., National Bureau of Economic Research.

Maehashia, K. and M. Shintani (2020): "Macroeconomic forecasting using factor models and machine learning: an application to Japan," *Journal of The Japanese and International Economies*, 58, 1–17.

Mian, A. R., L. Straub, and A. Sufi (2021): "What explains the decline in r*? Rising income inequality versus demographic shifts," *Rising Income Inequality Versus Demographic Shifts (September 22, 2021). University of Chicago, Becker Friedman Institute for Economics Working Paper*.

Miranda-Agrippino, S. and G. Ricco (2021): "The transmission of monetary policy shocks," *American Economic Journal: Macroeconomics*, 13, 74–107.

Moran, P. and A. Queralto (2018): "Innovation, productivity, and monetary policy," *Journal of Monetary Economics*, 93, 24–41.

Morley, J., T. D. Tran, and B. Wong (2024): "A simple correction for misspecification in trend-cycle decompositions with an application to estimating r," *Journal of Business & Economic Statistics*, 42, 665–680.

Morley, J. C., C. R. Nelson, and E. Zivot (2003): "Why Are the Beveridge–Nelson and Unobserved–Components Decompositions of GDP So Different?" *The Review of Economics and Statistics*, 85, 235–243.

Nakajima, J. (2023): "Estimation of firms' inflation expectations using the survey DI," Discussion Paper Series, Institute of Economic Research, Hitotsubashi University.

Nuño, G. (2025): "Three Theories of Natual Rate Dynamics," Banco de España Working Paper 2528, Banco de España.

Oh, K. H., E. Zivot, and D. Creal (2008): "The relationship between the Beveridge–Nelson decomposition and other permanent–transitory decompositions that are popular in economics," *Journal of Econometrics*, 146, 207–219.

Pagan, A. (1985): "Econometric Issues in the Analysis of Regressions with Generated Regressors," *International Economic Review*, 26, 221–247.

Ramey, V. A. (2016): "Macroeconomic Shocks and Their Propagation," *Handbook of Macroeconomics*, 2, 71–162.

Romer, C. D. and D. H. Romer (2004): "A new measure of monetary shocks: Derivation and implications," *American Economic Review*, 94, 1055–1084.

Rungcharoenkitkul, P. and F. Winkler (2025): "The natural rate of interest through a hall of mirrors," *Journal of Monetary Economics*, 103858.

Smets, F. and R. Wouters (2007): "Shocks and frictions in US business cycles: A Bayesian DSGE approach," *American Economic Review*, 97, 586–606.

Stadler, G. W. (1990): "Business cycle models with endogenous technology," *The American Economic Review*, 763–778.

Stock, J. H. and M. W. Watson (2007): "Why has U.S. inflation become harder to forecast?" *Journal of Money, Credit and Banking*, 39, 3–33.

Trenkler, C. and E. Weber (2016): "On the identification of multivariate correlated unobserved components models," *Economics Letters*, 138, 15–18.

Watson, M. W. (1986): "Univariate detrending methods with stochastic trends," *Journal of monetary economics*, 18, 49–75.

A Appendix

TABLE A-1: Data and Sample Periods for the Different Model Specifications

Model Specification (Sample)	Variable	Source
Benchmark (1989:Q1–2019:Q4)	CPI Inflation	FRED
	10-Year PCE Inflation Expectations	SPF & FRB
	3-Month T-Bill Yield	FRED
	10-Year T-Note Yield	FRED
	20-Year T-Bond Yield	FRED
	Bauer and Swanson Shocks	Bauer and Swanson (2023)
Rob. Shocks 1: Romer and Rommer (1985:Q1–2007:Q4)	Benchmark except shocks	FRED
	Romer and Romer Shocks	Romer and Romer (2004)
Rob. Shocks 2: Gertler and Karadi (1991:Q1–2012:Q2)	Benchmark except shocks	FRED
	Gertler and Karadi Shocks	Gertler and Karadi (2015)
Rob. Shocks 3: M-A and Ricco (1992:Q1–2009:Q4)	Benchmark except shocks	FRED
	M-A and Ricco Shocks	Miranda-Agrippino and Ricco (2021)
Rob. Shocks 4: Jarocinski and Karadi (1991:Q1–2016:Q4)	Benchmark except shocks	FRED
	Jarocinski and Karadi Shocks	Jarociński and Karadi (2020)
Rob. Spec. 1: Additional Shocks (1989:Q1–2019:Q4)	Variables in Benchmark Spec.	FRED
Rob. Spec. 2: Additional Controls (1989:Q1–2019:Q4)	Benchmark except CPI Inflation	FRED
	Core PCE Inflation	FRED
	Real GDP Growth	FRED
	Employment Growth	FRED
	Excess Bond Premium	Gilchrist and Zakrajšek (2012)
Int. Evidence 1: United Kingdom (2000:Q1–2025:Q1)	CPI Inflation	Bank of England
	5-Year Inflation Expectations	Bank of England
	Short-term Interest Rate	Bank of England
	10-Year Bond Yield	Bank of England
	20-Year Bond Yield	Bank of England
	Braun et al. Shocks	Braun et al. (2025)
Int. Evidence 2: Euro Area (2005:Q2–2024:Q2)	HICP Inflation	ECB Data Portal
	Long-Term Inflation Expectations	Consensus
	ECB Deposit Facility Rate	ECB Data Portal
	12-Year Bond Yield	ECB Data Portal
	28-Year Bond Yield	ECB Data Portal
	Jarosiński and Karadi shocks	Jarociński and Karadi (2020)
Int. Evidence 3: Canada (1991:Q1–2020:Q1)	CPI Inflation	Statistics Canada
	Inflation Expectations	Bank of Canada
	Bank Rate	Bank of Canada
	3-5 Years Bond Yield	Bank of Canada
	10+ Years Bond Yield	Bank of Canada
	Champagne and Sekkel Shocks	Champagne and Sekkel (2018)
Int. Evidence 4: Japan (1993:Q2–2020:Q1)	CPI Inflation	OECD Database
	5-Year Inflation Expectations	Nakajima (2023)
	Official Discount Rate	Maehashia and Shintani (2020)
	10-Year Bond Yield	Maehashia and Shintani (2020)
	Long-Term Prime Lending Rate	Maehashia and Shintani (2020)
	Kubota and Shintani Shocks	Kubota and Shintani (2022)

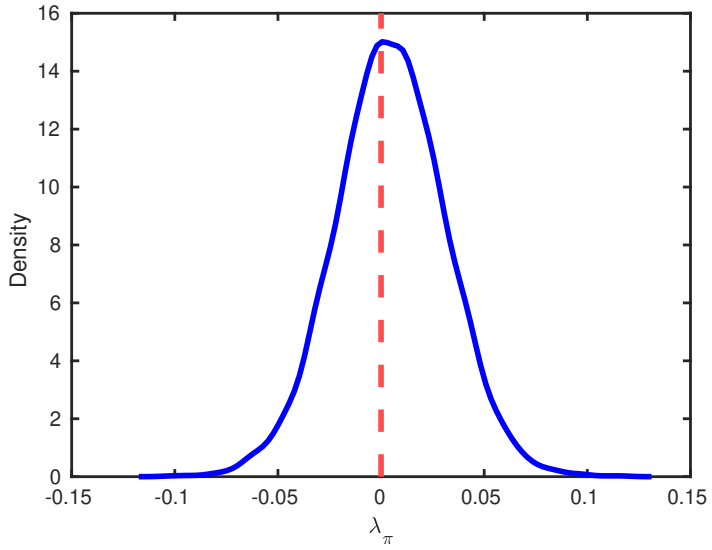
Note: The table reports sample periods, variables, and data sources used to estimate each model specification. "Benchmark" refers to the specification described in Section 2 for the U.S. economy. "Benchmark expect `X`" uses all Benchmark variables except `X`. Abbreviations: "Rob." = Robustness, "Spec." = Specification, "Int" = International, "FRED" = Federal Reserve Economic Data, "SPF" = Survey of Professional Forecasters, FRB = Federal Reserve Board, and "Shocks" = Monetary Policy Shocks. For U.S. inflation expectations, we use long-run PCE inflation expectations from the SPF from 2007 onward; before then, we rely on survey-based long-run (5- to 10-year) PCE inflation expectations from the FRB/U.S. model. For Canada, inflation expectations are a model-based long-term common index generated by Bank of Canada staff using a dynamic factor model.

TABLE A-2: Elasticity of r_t^* to Monetary Policy Shocks

Model Specification	λ_r Median	λ_r Percentiles [10^{th}, 90^{th}]
Benchmark	-0.16	$[-0.27, -0.06]$
Robustness Shocks 1: Romer and Romer	-0.06	$[-0.13, \quad 0.00]$
Robustness Shocks 2: Gertler and Karadi	-0.10	$[-0.24, -0.01]$
Robustness Shocks 3: Miranda-Agrippino and Ricco	-0.08	$[-0.19, \quad 0.01]$
Robustness Shocks 4: Jarocinski and Karadi	-0.09	$[-0.18, -0.02]$
Robustness Specification 1: Additional Shocks	-0.32	$[-0.46, -0.20]$
Robustness Specification 2: Additional Controls	-0.08	$[-0.16, -0.02]$
International Evidence 1: United Kingdom	-0.06	$[-0.13, -0.01]$
International Evidence 2: Euro Area	-0.04	$[-0.10, \quad 0.00]$
International Evidence 3: Canada	-0.02	$[-0.08, \quad 0.03]$
International Evidence 4: Japan	-0.09	$[-0.15, -0.04]$

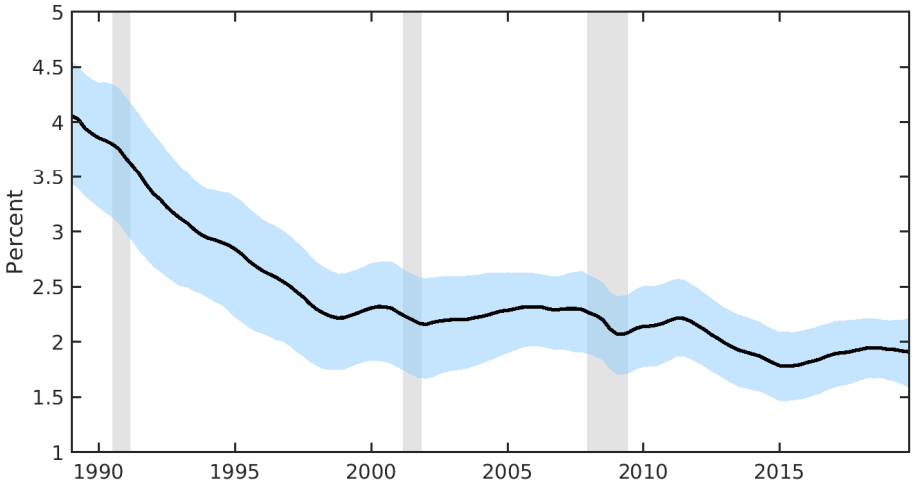
Note: The table reports the posterior median and the 10th and 90th percentiles of the distribution of the sensitivity (λ_r) of r_t^* to monetary policy shocks for each model specification.

FIGURE A-1: Elasticity of Trend Inflation to Monetary Policy Shocks



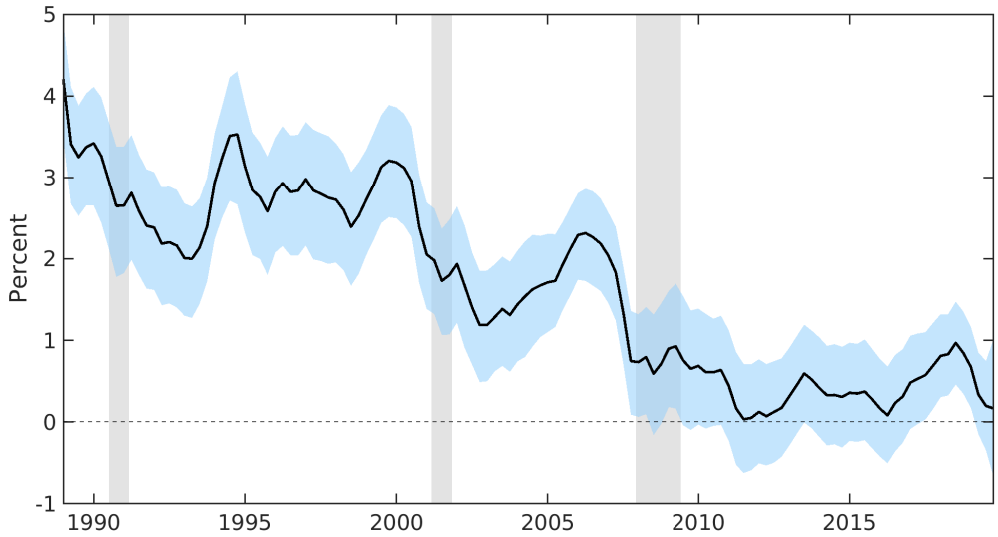
Note: The figure shows the posterior density of the sensitivity (λ_π) of trend inflation to monetary policy shocks, as defined in Equation (19). The vertical dashed red line denotes the prior mode of λ_π.

FIGURE A-2: Trend Inflation (π_t^*)



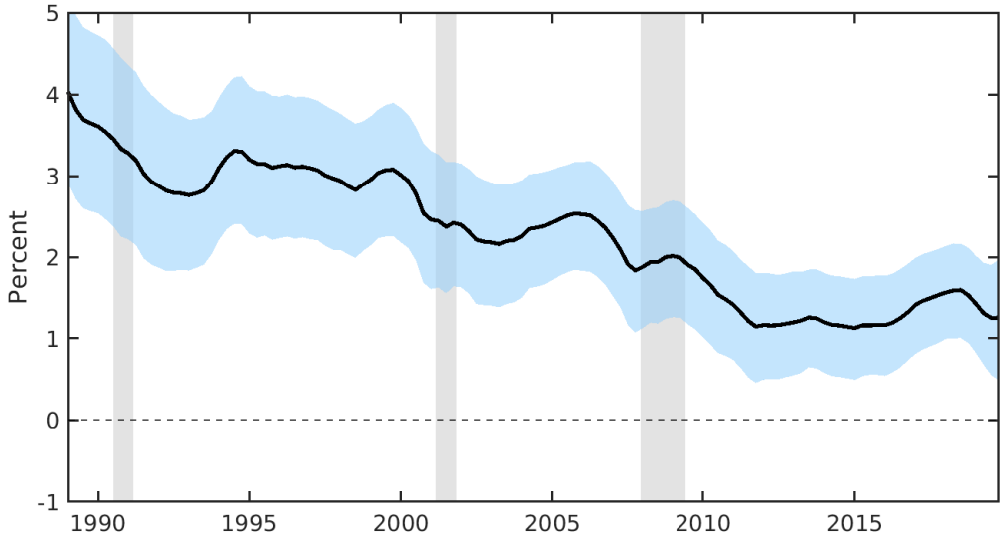
Note: The black line plots the posterior median of π_t^*. The light blue area shows the 90% credible set. The light gray vertical bars indicate NBER recession periods. The sample period is 1988:Q1–2019:Q4.

FIGURE A-3: r_t^* – Specification with Additional Shocks



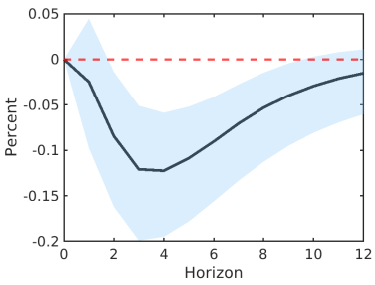
Note: The black line plots the posterior median of r_t^*. The light blue area shows the 90% credible set. The light gray vertical bars indicate NBER recession periods. The sample period is 1988:Q1–2019:Q4. The model corresponds to Robustness Specification 2: Additional Shocks, as defined in Table A-1.

FIGURE A-4: r_t^* – Specification with Additional Controls

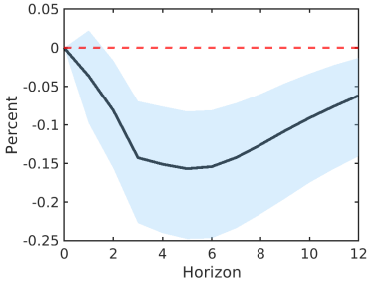


Note: The black line plots the posterior median of r_t^*. The light blue area shows the 90% credible set. The light gray vertical bars indicate NBER recession periods. The sample period is 1988:Q1–2019:Q4. The model corresponds to Robustness Specification 2: Additional Controls, as defined in Table A-1.

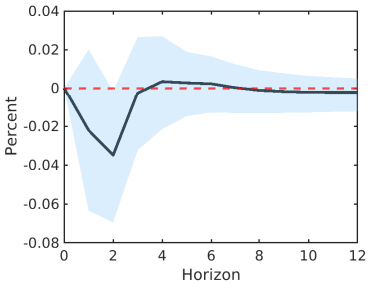
FIGURE A-5: Cyclical Effects of Monetary Policy Shocks



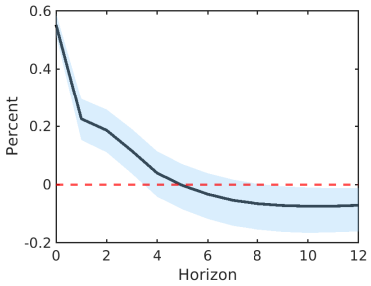
A. Real GDP Growth



B. Employment Growth



C. Core PCE Inflation



D. 3-Month T-Bill Yield

Note: The figure shows the response of macroeconomic variables to a 100 basis points monetary policy shock. Black lines indicate the posterior median, and light blue areas show the 16th and 84th percentiles. The horizon is in quarters. The responses are computed using the cyclical block (i.e., the stationary VAR component) of the TC-BVAR corresponding to Robustness Specification 2: Additional Controls, as defined in Table A-1.

Supplementary Materials

— For Online Publication Only —

Estimation Algorithm

Below we provide the details for the MCMC algorithm we use to estimate the baseline TC-BVAR in the main text. All extensions of the baseline setup considered in the paper are nested within, and can be easily accommodated by, the same six-step MCMC algorithm described in this section. For convenience, below we reproduce the six conditional posterior densities shown in Section 2.4.

$$(1)\ \boldsymbol{\tau} \mid \widetilde{\mathbf{y}},\ \boldsymbol{\theta} \sim \mathcal{N}\big(\overline{\mathbf{d}}_{\tau},\ \overline{\mathbf{D}}_{\tau}\big),$$

$$(2)\ \boldsymbol{\beta} \mid \widetilde{\mathbf{y}},\ \boldsymbol{\tau},\ \boldsymbol{\theta}_{-\beta} \sim \mathcal{N}\big(\overline{\mathbf{d}}_{\beta},\ \overline{\mathbf{D}}_{\beta}\big),$$

$$(3)\ \boldsymbol{\alpha}_i \mid \widetilde{\mathbf{y}},\ \boldsymbol{\tau},\ \boldsymbol{\theta}_{-\alpha_i} \sim \mathcal{N}\big(\overline{d}_{\alpha_i},\ \overline{D}_{\alpha_i}\big), \qquad i = 2, \ldots, N+1,$$

$$(4)\ \boldsymbol{\sigma}^2_{\tilde{e},i} \mid \widetilde{\mathbf{y}},\ \boldsymbol{\tau},\ \boldsymbol{\theta}_{-\sigma^2_{\tilde{e},i}} \sim \mathcal{IG}\big(\overline{v}_{\tilde{e},i},\ \overline{S}_{\tilde{e},i}\big), \qquad i = 1, \ldots, N+1,$$

$$(5)\ \boldsymbol{\sigma}^2_{\xi^*,k} \mid \widetilde{\mathbf{y}},\ \boldsymbol{\tau},\ \boldsymbol{\theta}_{-\sigma^2_{\xi^*,k}} \sim \mathcal{IG}\big(\overline{v}_{\xi^*,k},\ \overline{S}_{\xi^*,k}\big), \qquad k \in \{\pi^*,\ r^*\},$$

$$(6)\ \boldsymbol{\lambda} \mid \widetilde{\mathbf{y}},\ \boldsymbol{\tau},\ \boldsymbol{\theta}_{-\lambda} \sim \mathcal{N}\big(\overline{\mathbf{d}}_{\lambda},\ \overline{\mathbf{D}}_{\lambda}\big),$$

where $\boldsymbol{\theta}_{-\ell}$ denotes the parameter set $\boldsymbol{\theta}$ with element ℓ removed.

We derive an estimation algorithm based on a stack representation of the TC-BVAR in (21)–(23):

$$\widetilde{\mathbf{y}} = \mathbf{W}\boldsymbol{\tau} + \mathbf{X}\boldsymbol{\beta} + \mathbf{G}\tilde{\mathbf{e}}, \tag{A-1}$$

$$\mathbf{L}_{\boldsymbol{\tau}}\boldsymbol{\tau} = \boldsymbol{\tau}_0 + \mathbf{L}_{\boldsymbol{\lambda}}\tilde{\mathbf{e}} + \mathbf{L}_{\boldsymbol{\Sigma}_{\tilde{\xi}}}\widetilde{\boldsymbol{\xi}}^*, \tag{A-2}$$

where the stacked vectors are defined as:

$$\widetilde{\mathbf{y}} = \begin{bmatrix}\widetilde{\mathbf{y}}_1' & \cdots & \widetilde{\mathbf{y}}_T'\end{bmatrix}', \qquad \boldsymbol{\tau} = \begin{bmatrix}\boldsymbol{\tau}_1' & \cdots & \boldsymbol{\tau}_T'\end{bmatrix}', \qquad \tilde{\mathbf{e}} = \begin{bmatrix}\tilde{\mathbf{e}}_1' & \cdots & \tilde{\mathbf{e}}_T'\end{bmatrix}', \qquad \widetilde{\boldsymbol{\xi}}^* = \begin{bmatrix}\widetilde{\boldsymbol{\xi}}_1^{*\prime} & \cdots & \widetilde{\boldsymbol{\xi}}_T^{*\prime}\end{bmatrix}',$$

with $\widetilde{\mathbf{y}}_t$ being of dimension $(N+1) \times 1$ and $\boldsymbol{\tau}_t$ of dimension 2×1.

Moreover, $\boldsymbol{\tau}_0$ is a $2T \times 1$ vector of initial conditions defined as:

$$\boldsymbol{\tau}_0 = \left(\begin{bmatrix}\pi_0^* \\ r_0^*\end{bmatrix} \otimes \begin{bmatrix}1 \\ 0 \\ \vdots \\ 0\end{bmatrix} \right), \tag{A-3}$$

where π_0^* and r_0^* denote the initial values of trend inflation and the natural rate of interest, respec-

tively.[23]

Furthermore, the system matrices are given by:

$$\mathbf{W} = I_T \otimes S,\ \mathbf{X} = \begin{bmatrix} X_1 \\ X_2 \\ \vdots \\ X_T \end{bmatrix},\ X_t = I_{N+1} \otimes ((\mathbf{y}_{t-1} - S\boldsymbol{\tau}_{t-1})' \cdots (\mathbf{y}_{t-p} - S\boldsymbol{\tau}_{t-p})')$$

$$\mathbf{G} = \mathbf{L}_{\mathbf{A}}\mathbf{L}_{\boldsymbol{\Sigma}_{\tilde{e}}},\ \mathbf{L}_{\mathbf{A}} = I_T \otimes A,\ \mathbf{L}_{\boldsymbol{\Sigma}_{\tilde{e}}} = I_T \otimes \boldsymbol{\Sigma}_{\tilde{e}}^{1/2},\ \mathbf{L}_{\boldsymbol{\tau}} = \begin{bmatrix} I_2 & \mathbf{0}_{2\times 2} & \cdots & & \mathbf{0}_{2\times 2} \\ -I_2 & I_2 & & & \\ \mathbf{0}_{2\times 2} & -I_2 & \ddots & & \vdots \\ \vdots & & \ddots & & \\ \mathbf{0}_{2\times 2} & & & -I_2 & I_2 \end{bmatrix},\ \text{and}$$

$\mathbf{L}_{\boldsymbol{\lambda}} = I_T \otimes H_\lambda$.

- *Sampling* $\boldsymbol{\tau}$

Note that, by a simple change of variable: $\widetilde{\boldsymbol{\tau}} = \mathbf{L}_{\boldsymbol{\tau}}\boldsymbol{\tau}$ and $\mathbf{W}\boldsymbol{\tau} = \widetilde{\mathbf{W}}\widetilde{\boldsymbol{\tau}}$, where $\widetilde{\mathbf{W}} = \mathbf{W}\mathbf{L}_{\boldsymbol{\tau}}^{-1}$, (A-1) and (A-2) can be equivalently represented as:

$$\widetilde{\mathbf{y}} = \widetilde{\mathbf{W}}\widetilde{\boldsymbol{\tau}} + \mathbf{X}\boldsymbol{\beta} + \mathbf{G}\tilde{\mathbf{e}}, \tag{A-4}$$

$$\widetilde{\boldsymbol{\tau}} = \boldsymbol{\tau}_0 + \mathbf{L}_{\boldsymbol{\lambda}}\tilde{\mathbf{e}} + \mathbf{L}_{\boldsymbol{\Sigma}_{\tilde{\xi}}}\widetilde{\boldsymbol{\xi}}^*. \tag{A-5}$$

For notational convenience, in what follows, we derive the full conditional posterior for $\widetilde{\boldsymbol{\tau}}$. Of course, given a draw for $\widetilde{\boldsymbol{\tau}}$, recovering $\boldsymbol{\tau}$ is straightforward by simply setting $\boldsymbol{\tau} = \mathbf{L}_{\boldsymbol{\tau}}^{-1}\widetilde{\boldsymbol{\tau}}$.

To sample $\widetilde{\boldsymbol{\tau}}$, one first needs to obtain an expression for the likelihood function, $\mathcal{L}(\widetilde{\boldsymbol{\tau}}, \boldsymbol{\theta}|\widetilde{\mathbf{y}}) = f(\widetilde{\mathbf{y}}|\widetilde{\boldsymbol{\tau}}, \boldsymbol{\theta})$, and the prior density, $f(\widetilde{\boldsymbol{\tau}}|\boldsymbol{\theta})$. The prior can be readily obtained from (A-5):

$$\widetilde{\boldsymbol{\tau}}|\boldsymbol{\theta} \sim \mathcal{N}(\boldsymbol{\mu}_{\widetilde{\boldsymbol{\tau}}},\ \boldsymbol{\Sigma}_{\widetilde{\boldsymbol{\tau}}\widetilde{\boldsymbol{\tau}}}), \tag{A-6}$$

where the first and second moments – conditional on $\boldsymbol{\theta}$ – in (A-6) are respectively given by:[24]

$$\boldsymbol{\mu}_{\widetilde{\boldsymbol{\tau}}} = \mathbb{E}\left(\boldsymbol{\tau}_0 + \mathbf{L}_{\boldsymbol{\lambda}}\tilde{\mathbf{e}} + \mathbf{L}_{\boldsymbol{\Sigma}_{\tilde{\xi}}}\widetilde{\boldsymbol{\xi}}^*\right) = \boldsymbol{\tau}_0, \tag{A-7}$$

$$\boldsymbol{\Sigma}_{\widetilde{\boldsymbol{\tau}}\widetilde{\boldsymbol{\tau}}} = \mathbb{V}\text{ar}\left(\mathbf{L}_{\boldsymbol{\lambda}}\tilde{\mathbf{e}} + \mathbf{L}_{\boldsymbol{\Sigma}_{\tilde{\xi}}}\widetilde{\boldsymbol{\xi}}^*\right) = \mathbf{L}_{\boldsymbol{\lambda}}\mathbb{V}\text{ar}(\tilde{\mathbf{e}})\mathbf{L}_{\boldsymbol{\lambda}}' + \mathbf{L}_{\boldsymbol{\Sigma}_{\tilde{\xi}}}\mathbb{V}\text{ar}(\widetilde{\boldsymbol{\xi}}^*)\mathbf{L}_{\boldsymbol{\Sigma}_{\tilde{\xi}}}' = \mathbf{L}_{\boldsymbol{\lambda}}\mathbf{L}_{\boldsymbol{\lambda}}' + \mathbf{L}_{\boldsymbol{\Sigma}_{\tilde{\xi}}}\mathbf{L}_{\boldsymbol{\Sigma}_{\tilde{\xi}}}'. \tag{A-8}$$

Next, using the properties of the Normal distribution (see, e.g., Theorem 3.8 in Kroese and Chan

[23] In practice, we initialize π_0^* and r_0^* using the pre-sample three-decade averages of CPI inflation and the short-term nominal interest rate, respectively.

[24] To make notation less cumbersome – while explicitly mentioning what they are — we omit conditional factors in the expressions for expectation, variance and covariance operators.

(2014), chapter 3.6) the likelihood function $f(\widetilde{\mathbf{y}}|\widetilde{\boldsymbol{\tau}},\boldsymbol{\theta})$ is given by:

$$\widetilde{\mathbf{y}}|\widetilde{\boldsymbol{\tau}},\boldsymbol{\theta} \sim \mathcal{N}\left(\boldsymbol{\mu}_{\mathbf{y}} + \boldsymbol{\Sigma}'_{\widetilde{\boldsymbol{\tau}}\mathbf{y}}\boldsymbol{\Sigma}^{-1}_{\widetilde{\boldsymbol{\tau}}\widetilde{\boldsymbol{\tau}}}\left(\widetilde{\boldsymbol{\tau}} - \boldsymbol{\mu}_{\widetilde{\boldsymbol{\tau}}}\right),\ \boldsymbol{\Sigma}_{\mathbf{yy}} - \boldsymbol{\Sigma}'_{\widetilde{\boldsymbol{\tau}}\mathbf{y}}\boldsymbol{\Sigma}^{-1}_{\widetilde{\boldsymbol{\tau}}\widetilde{\boldsymbol{\tau}}}\boldsymbol{\Sigma}_{\widetilde{\boldsymbol{\tau}}\mathbf{y}}\right). \tag{A-9}$$

The expression above introduces three new terms, $\boldsymbol{\mu}_{\mathbf{y}}$, $\boldsymbol{\Sigma}_{\mathbf{yy}}$ and $\boldsymbol{\Sigma}_{\widetilde{\boldsymbol{\tau}}\mathbf{y}}$. The first two denote first and second moments, respectively, which – conditional on $\widetilde{\boldsymbol{\tau}}$ and $\boldsymbol{\theta}$ – are obtained from the measurement equation in (A-4). Specifically, we have:

$$\boldsymbol{\mu}_{\mathbf{y}} = \mathbb{E}\left(\widetilde{\mathbf{W}}\widetilde{\boldsymbol{\tau}} + \mathbf{X}\boldsymbol{\beta} + \mathbf{G}\tilde{\mathbf{e}}\right) = \widetilde{\mathbf{W}}\widetilde{\boldsymbol{\tau}} + \mathbf{X}\boldsymbol{\beta}, \tag{A-10}$$

$$\boldsymbol{\Sigma}_{\mathbf{yy}} = \mathbb{V}\mathrm{ar}\left(\mathbf{G}\tilde{\mathbf{e}}\right) = \mathbf{G}\mathbb{V}\mathrm{ar}(\tilde{\mathbf{e}})\mathbf{G}' = \mathbf{G}\mathbf{G}'. \tag{A-11}$$

The cross-covariance term, $\boldsymbol{\Sigma}_{\widetilde{\boldsymbol{\tau}}\mathbf{y}}$, appears in (A-9) since the vector of cyclical disturbances ($\tilde{\mathbf{e}}$) is a common driver to both $\widetilde{\mathbf{y}}$ and the trend-vector $\widetilde{\boldsymbol{\tau}}$. Therefore, from (A-4) and (A-5) and recalling $\tilde{\mathbf{e}}$ and $\widetilde{\boldsymbol{\xi}}^*$ are independent random vectors, we have:

$$\boldsymbol{\Sigma}_{\widetilde{\boldsymbol{\tau}}\mathbf{y}} = \mathbb{C}\mathrm{ov}\left(\mathbf{L}_{\boldsymbol{\lambda}}\tilde{\mathbf{e}},\ \mathbf{G}\tilde{\mathbf{e}}\right) = \mathbf{L}_{\boldsymbol{\lambda}}\mathbb{C}\mathrm{ov}\left(\tilde{\mathbf{e}},\ \tilde{\mathbf{e}}\right)\mathbf{G}' = \mathbf{L}_{\boldsymbol{\lambda}}\mathbb{V}\mathrm{ar}(\tilde{\mathbf{e}})\mathbf{G}' = \mathbf{L}_{\boldsymbol{\lambda}}\mathbf{G}'. \tag{A-12}$$

Of course, in the absence of endogenous time variation, $\mathbf{L}_{\boldsymbol{\lambda}}$ is a null matrix and so is $\boldsymbol{\Sigma}_{\widetilde{\boldsymbol{\tau}}\mathbf{y}}$, which returns an expression for (A-9) that is consistent with the likelihood function for the standard orthogonal-component TC-BVAR.[25]

Finally, applying Bayes' rule to combine (A-6) and (A-9) and using the results in (A-7)-(A-8), (A-10)-(A-11) and (A-12) yields:

$$\begin{aligned}
f(\widetilde{\boldsymbol{\tau}}|\widetilde{\mathbf{y}},\boldsymbol{\theta}) &\propto f(\widetilde{\mathbf{y}}|\widetilde{\boldsymbol{\tau}},\boldsymbol{\theta})f(\widetilde{\boldsymbol{\tau}}|\boldsymbol{\theta}),\\
&\propto \exp\left[-\frac{\left(\mathbf{y}_* - \mathbf{B}\widetilde{\boldsymbol{\tau}}\right)'\mathbf{K}_{\mathbf{y}}{}^{-1}\left(\mathbf{y}_* - \mathbf{B}\widetilde{\boldsymbol{\tau}}\right) + \left(\widetilde{\boldsymbol{\tau}} - \boldsymbol{\tau}_0\right)'\boldsymbol{\Sigma}^{-1}_{\widetilde{\boldsymbol{\tau}}\widetilde{\boldsymbol{\tau}}}\left(\widetilde{\boldsymbol{\tau}} - \boldsymbol{\tau}_0\right)}{2}\right],\\
&\propto \exp\left[-\frac{\widetilde{\boldsymbol{\tau}}'\left(\mathbf{B}'\mathbf{K}_{\mathbf{y}}{}^{-1}\mathbf{B} + \left(\mathbf{L}_{\boldsymbol{\lambda}}\mathbf{L}'_{\boldsymbol{\lambda}} + \mathbf{L}_{\boldsymbol{\Sigma}_{\tilde{\xi}}}\mathbf{L}'_{\boldsymbol{\Sigma}_{\tilde{\xi}}}\right)^{-1}\right)\widetilde{\boldsymbol{\tau}} - 2\left(\mathbf{y}_*{}'\mathbf{K}_{\mathbf{y}}{}^{-1}\mathbf{B} + \boldsymbol{\tau}'_0\left(\mathbf{L}_{\boldsymbol{\lambda}}\mathbf{L}'_{\boldsymbol{\lambda}} + \mathbf{L}_{\boldsymbol{\Sigma}_{\tilde{\xi}}}\mathbf{L}'_{\boldsymbol{\Sigma}_{\tilde{\xi}}}\right)^{-1}\right)\widetilde{\boldsymbol{\tau}}}{2}\right],
\end{aligned} \tag{A-13}$$

where we define:

$$\begin{aligned}
\mathbf{y}_* &= \widetilde{\mathbf{y}} - \mathbf{X}\boldsymbol{\beta} + \boldsymbol{\Sigma}'_{\widetilde{\boldsymbol{\tau}}\widetilde{\mathbf{y}}}\boldsymbol{\Sigma}^{-1}_{\widetilde{\boldsymbol{\tau}}\widetilde{\boldsymbol{\tau}}}\boldsymbol{\mu}_{\widetilde{\boldsymbol{\tau}}} = \widetilde{\mathbf{y}} - \mathbf{X}\boldsymbol{\beta} + \mathbf{G}\mathbf{L}'_{\boldsymbol{\lambda}}\left(\mathbf{L}_{\boldsymbol{\lambda}}\mathbf{L}'_{\boldsymbol{\lambda}} + \mathbf{L}_{\boldsymbol{\Sigma}_{\tilde{\xi}}}\mathbf{L}'_{\boldsymbol{\Sigma}_{\tilde{\xi}}}\right)^{-1}\boldsymbol{\tau}_0,\\
\mathbf{B} &= \widetilde{\mathbf{W}} + \boldsymbol{\Sigma}'_{\widetilde{\boldsymbol{\tau}}\widetilde{\mathbf{y}}}\boldsymbol{\Sigma}^{-1}_{\widetilde{\boldsymbol{\tau}}\widetilde{\boldsymbol{\tau}}} = \widetilde{\mathbf{W}} + \mathbf{G}\mathbf{L}'_{\boldsymbol{\lambda}}\left(\mathbf{L}_{\boldsymbol{\lambda}}\mathbf{L}'_{\boldsymbol{\lambda}} + \mathbf{L}_{\boldsymbol{\Sigma}_{\tilde{\xi}}}\mathbf{L}'_{\boldsymbol{\Sigma}_{\tilde{\xi}}}\right)^{-1},\\
\mathbf{K}_{\mathbf{y}} &= \boldsymbol{\Sigma}_{\widetilde{\mathbf{y}}\widetilde{\mathbf{y}}} - \boldsymbol{\Sigma}'_{\widetilde{\boldsymbol{\tau}}\widetilde{\mathbf{y}}}\boldsymbol{\Sigma}^{-1}_{\widetilde{\boldsymbol{\tau}}\widetilde{\boldsymbol{\tau}}}\boldsymbol{\Sigma}_{\widetilde{\boldsymbol{\tau}}\widetilde{\mathbf{y}}} = \mathbf{G}\mathbf{G}' - \mathbf{G}\mathbf{L}'_{\boldsymbol{\lambda}}\left(\mathbf{L}_{\boldsymbol{\lambda}}\mathbf{L}'_{\boldsymbol{\lambda}} + \mathbf{L}_{\boldsymbol{\Sigma}_{\tilde{\xi}}}\mathbf{L}'_{\boldsymbol{\Sigma}_{\tilde{\xi}}}\right)^{-1}\mathbf{L}_{\boldsymbol{\lambda}}\mathbf{G}'.
\end{aligned}$$

[25] A similar rationale applies for the prior variance-covariance matrix $\boldsymbol{\Sigma}_{\widetilde{\boldsymbol{\phi}}\widetilde{\boldsymbol{\phi}}}$ in (A-8).

The expression in (A-13) reveals a Gaussian kernel such that:

$$\widetilde{\boldsymbol{\tau}}|\widetilde{\mathbf{y}},\boldsymbol{\theta} \sim \mathcal{N}\left(\overline{\mathbf{d}}_{\widetilde{\tau}},\ \overline{\mathbf{D}}_{\widetilde{\tau}}\right), \text{ where } \begin{cases} \overline{\mathbf{d}}_{\widetilde{\tau}} = \overline{\mathbf{D}}_{\widetilde{\tau}}\left(\mathbf{B}'{\mathbf{K}_{\mathbf{y}}}^{-1}\mathbf{y}_{*} + \left(\mathbf{L}_{\boldsymbol{\lambda}}\mathbf{L}_{\boldsymbol{\lambda}}' + \mathbf{L}_{\boldsymbol{\Sigma}_{\tilde{\xi}}}\mathbf{L}_{\boldsymbol{\Sigma}_{\tilde{\xi}}}'\right)^{-1}\boldsymbol{\tau}_0\right), \\ \overline{\mathbf{D}}_{\widetilde{\tau}} = \left(\mathbf{B}'{\mathbf{K}_{\mathbf{y}}}^{-1}\mathbf{B} + \left(\mathbf{L}_{\boldsymbol{\lambda}}\mathbf{L}_{\boldsymbol{\lambda}}' + \mathbf{L}_{\boldsymbol{\Sigma}_{\tilde{\xi}}}\mathbf{L}_{\boldsymbol{\Sigma}_{\tilde{\xi}}}'\right)^{-1}\right)^{-1}. \end{cases} \tag{A-14}$$

To produce draws for $\widetilde{\boldsymbol{\tau}}|\widetilde{\mathbf{y}},\boldsymbol{\theta}$ one needs to construct $\overline{\mathbf{d}}_{\widetilde{\tau}}$ and $\overline{\mathbf{D}}_{\widetilde{\tau}}$. This can be done using the posterior simulation algorithm of Chan and Jeliazkov (2009). As mentioned earlier, draws for $\boldsymbol{\tau}|\widetilde{\mathbf{y}},\boldsymbol{\theta}$ can then be recovered by simply computing $\boldsymbol{\tau} = \mathbf{L}^{-1}\widetilde{\boldsymbol{\tau}}$.

• *Sampling* $\boldsymbol{\beta}$

Recall the stacked measurement equation of the TC-BVAR,

$$\widetilde{\mathbf{y}} = \mathbf{W}\boldsymbol{\tau} + \mathbf{X}\boldsymbol{\beta} + \mathbf{G}\tilde{\mathbf{e}}. \tag{A-15}$$

Conditional on $(\boldsymbol{\tau}, \boldsymbol{\theta}_{-\beta})$, define

$$\mathbf{y}_{\beta} \equiv \widetilde{\mathbf{y}} - \mathbf{W}\boldsymbol{\tau}, \tag{A-16}$$

so that (A-15) can be rewritten as

$$\mathbf{y}_{\beta} = \mathbf{X}\boldsymbol{\beta} + \mathbf{G}\tilde{\mathbf{e}}, \qquad \tilde{\mathbf{e}} \sim \mathcal{N}(\mathbf{0}, I_{(N+1)T}). \tag{A-17}$$

Hence,

$$\mathbf{y}_{\beta} \mid \boldsymbol{\beta}, \boldsymbol{\tau}, \boldsymbol{\theta}_{-\beta} \sim \mathcal{N}\left(\mathbf{X}\boldsymbol{\beta},\ \mathbf{G}\mathbf{G}'\right). \tag{A-18}$$

We assume a Minnesota-type Gaussian prior centered at zero,

$$\boldsymbol{\beta} \sim \mathcal{N}(\mathbf{0},\ \mathbf{D}_{\beta}), \tag{A-19}$$

where $\mathbf{D}_{\beta}$ is a block-diagonal prior covariance matrix which imposes lag-decaying shrinkage as in Giannone et al. (2015). In particular, partition $\boldsymbol{\beta}$ equation-by-equation as

$$\boldsymbol{\beta} = \begin{bmatrix} \boldsymbol{\beta}_1' & \cdots & \boldsymbol{\beta}_N' \end{bmatrix}', \qquad \boldsymbol{\beta}_i = \begin{bmatrix} \Phi_{i,1}' & \cdots & \Phi_{i,p}' \end{bmatrix}', \qquad i = 1, \ldots, N, \tag{A-20}$$

where $\Phi_{i,j}$ denotes the i^{th} row of the j^{th} lag matrix Φ_j. Since each $\Phi_{i,j}$ is a $1 \times N$ vector, $\boldsymbol{\beta}_i$ is of dimension $(Np) \times 1$.

The prior covariance matrix is block diagonal across equations,

$$\mathbf{D}_{\beta} = \mathtt{diag}(\mathbf{D}_{\beta_1}, \ldots, \mathbf{D}_{\beta_N}), \tag{A-21}$$

with each block $\mathbf{D}_{\beta_i}$ admitting the lag-block structure

$$\mathbf{D}_{\beta_i} = \texttt{diag}(\mathbf{D}_{\beta_i,1}, \ldots, \mathbf{D}_{\beta_i,p}), \qquad i = 1, \ldots, N, \tag{A-22}$$

where $\mathbf{D}_{\beta_i,j}$ is the $N \times N$ prior covariance matrix associated with the coefficients in $\Phi_{i,j}$.

Following Giannone et al. (2015), lag-decaying shrinkage is implemented through an overall tightness parameter γ such that

$$\mathbf{D}_{\beta_i,j} = \gamma \left(\frac{1}{j}\right) I_N, \qquad j = 1, \ldots, p, \qquad \gamma = 0.2. \tag{A-23}$$

Therefore, the prior variance of autoregressive coefficients decreases with the lag order, implying stronger shrinkage towards zero at longer horizons.

Finally, we impose stationarity of the cyclical VAR component. Let $\mathbb{I}(\mathcal{S}(\boldsymbol{\beta}))$ denote an indicator function which equals one if the companion form implied by $\boldsymbol{\beta}$ satisfies the stationarity condition (i.e., all eigenvalues lie strictly inside the unit circle), and equals zero otherwise. Therefore, the conditional posterior is truncated to the stationary region.

Combining likelihood and prior, the kernel of the conditional posterior density is given by

$$\begin{aligned} f(\boldsymbol{\beta} \mid \widetilde{\mathbf{y}}, \boldsymbol{\tau}, \boldsymbol{\theta}_{-\beta}) &\propto f(\mathbf{y}_\beta \mid \boldsymbol{\beta}, \boldsymbol{\tau}, \boldsymbol{\theta}_{-\beta}) f(\boldsymbol{\beta}) \mathbb{I}(\mathcal{S}(\boldsymbol{\beta})) \\ &\propto \exp\left[-\frac{(\mathbf{y}_\beta - \mathbf{X}\boldsymbol{\beta})' (\mathbf{G}\mathbf{G}')^{-1} (\mathbf{y}_\beta - \mathbf{X}\boldsymbol{\beta}) + \boldsymbol{\beta}' \mathbf{D}_\beta^{-1} \boldsymbol{\beta}}{2}\right] \mathbb{I}(\mathcal{S}(\boldsymbol{\beta})) \\ &\propto \exp\left[-\frac{\boldsymbol{\beta}' \left(\mathbf{X}' (\mathbf{G}\mathbf{G}')^{-1} \mathbf{X} + \mathbf{D}_\beta^{-1}\right) \boldsymbol{\beta} - 2\boldsymbol{\beta}' \mathbf{X}' (\mathbf{G}\mathbf{G}')^{-1} \mathbf{y}_\beta}{2}\right] \mathbb{I}(\mathcal{S}(\boldsymbol{\beta})). \end{aligned} \tag{A-24}$$

The expression in (A-24) reveals a Gaussian kernel such that

$$\boldsymbol{\beta} \mid \widetilde{\mathbf{y}}, \boldsymbol{\tau}, \boldsymbol{\theta}_{-\beta} \sim \mathcal{N}\left(\overline{\mathbf{d}}_\beta,\ \overline{\mathbf{D}}_\beta\right) \mathbb{I}(\mathcal{S}(\boldsymbol{\beta})), \text{ where } \begin{cases} \overline{\mathbf{d}}_\beta = \overline{\mathbf{D}}_\beta \mathbf{X}' (\mathbf{G}\mathbf{G}')^{-1} \mathbf{y}_\beta, \\ \overline{\mathbf{D}}_\beta = \left(\mathbf{X}' (\mathbf{G}\mathbf{G}')^{-1} \mathbf{X} + \mathbf{D}_\beta^{-1}\right)^{-1}. \end{cases} \tag{A-25}$$

Therefore, in practice we first draw $\boldsymbol{\beta}$ from the Gaussian density in (A-25) and retain the draw if and only if $\mathbb{I}(\mathcal{S}(\boldsymbol{\beta})) = 1$, that is, if the implied cyclical VAR dynamics are stationary.

- *Sampling* $\boldsymbol{\alpha}_i$, $i = 2, \ldots, N+1$

Recall that the measurement equation of the TC-BVAR is

$$\widetilde{\mathbf{y}}_t = S\boldsymbol{\tau}_t + X_t \boldsymbol{\beta} + A \boldsymbol{\Sigma}_{\tilde{e}}^{1/2} \tilde{\mathbf{e}}_t, \qquad t = 1, \ldots, T, \tag{A-26}$$

where $\widetilde{\mathbf{y}}_t$ is of dimension $(N+1) \times 1$, with the last element corresponding to the monetary policy

proxy z_t. The impact matrix A is lower triangular with ones on the main diagonal, but its last row is subject to exclusion restrictions as discussed in the main text.

Define reduced-form residuals

$$\mathbf{u}_t \equiv \widetilde{\mathbf{y}}_t - S\boldsymbol{\tau}_t - X_t\boldsymbol{\beta}, \tag{A-27}$$

so that

$$\mathbf{u}_t = A\boldsymbol{\Sigma}_{\tilde{e}}^{1/2}\tilde{\mathbf{e}}_t. \tag{A-28}$$

Let α_i collect the free parameters in the i-th row of A, for $i = 2, \ldots, N+1$. For $i = 2, \ldots, N$, define

$$\alpha_i = \begin{bmatrix} a_{i1} & \cdots & a_{i,i-1} \end{bmatrix}', \tag{A-29}$$

while the first equation contains no unknown coefficients.

The $(N+1)$-th equation (corresponding to the proxy z_t) is subject to zero restrictions such that only the structural shock to the short-term nominal interest rate loads onto the proxy. In particular, the last row of A is given by

$$A_{N+1,\cdot} = \begin{bmatrix} 0 & 0 & \alpha_{N+1} & 0 & \cdots & 0 & 1 \end{bmatrix}, \tag{A-30}$$

so that α_{N+1} is scalar, with $\alpha_{N+1} = \alpha_z$.

For $i = 2, \ldots, N$, the i-th structural equation can be written as

$$u_{i,t} = \sum_{k=1}^{i-1} a_{ik}\sigma_{\tilde{e},k}\tilde{e}_{k,t} + \sigma_{\tilde{e},i}\tilde{e}_{i,t}. \tag{A-31}$$

Stacking over $t = 1, \ldots, T$, define

$$\mathbf{u}_i = \begin{bmatrix} u_{i,1} \\ \vdots \\ u_{i,T} \end{bmatrix}, \qquad \mathbf{Z}_i = \begin{bmatrix} \sigma_{\tilde{e},1}\tilde{e}_{1,1} & \cdots & \sigma_{\tilde{e},i-1}\tilde{e}_{i-1,1} \\ \vdots & & \vdots \\ \sigma_{\tilde{e},1}\tilde{e}_{1,T} & \cdots & \sigma_{\tilde{e},i-1}\tilde{e}_{i-1,T} \end{bmatrix}, \tag{A-32}$$

$$\boldsymbol{\varepsilon}_i = \begin{bmatrix} \sigma_{\tilde{e},i}\tilde{e}_{i,1} \\ \vdots \\ \sigma_{\tilde{e},i}\tilde{e}_{i,T} \end{bmatrix}, \qquad \boldsymbol{\varepsilon}_i \sim \mathcal{N}(\mathbf{0}, \sigma_{\tilde{e},i}^2 I_T). \tag{A-33}$$

The i-th equation admits the regression form

$$\mathbf{u}_i = \mathbf{Z}_i\alpha_i + \boldsymbol{\varepsilon}_i, \qquad i = 2, \ldots, N. \tag{A-34}$$

For the proxy equation ($i = N+1$), define

$$\mathbf{u}_{N+1} = \alpha_{N+1}\mathbf{z}_{N+1} + \boldsymbol{\varepsilon}_{N+1}, \qquad \boldsymbol{\varepsilon}_{N+1} \sim \mathcal{N}(\mathbf{0}, \sigma^2_{\tilde{e},N+1} I_T), \tag{A-35}$$

where $\mathbf{z}_{N+1}$ stacks the appropriately scaled short-term interest rate shock.

We assume Gaussian priors

$$\alpha_i \sim \mathcal{N}(\mathbf{d}_{\alpha_i},\ \mathbf{D}_{\alpha_i}), \qquad i = 2, \ldots, N+1, \tag{A-36}$$

where we set $\mathbf{d}_{\alpha_i} = 0$ and $\mathbf{D}_{\alpha_i}$ to be an identity matrix.

Combining likelihood and prior, the kernel of the conditional posterior density is Gaussian. Hence, for each $i = 2, \ldots, N+1$,

$$\alpha_i \mid \widetilde{\mathbf{y}}, \boldsymbol{\tau}, \boldsymbol{\theta}_{-\alpha_i} \sim \mathcal{N}\left(\overline{\mathbf{d}}_{\alpha_i},\ \overline{\mathbf{D}}_{\alpha_i}\right), \text{ where } \begin{cases} \overline{\mathbf{d}}_{\alpha_i} = \overline{\mathbf{D}}_{\alpha_i}\left(\mathbf{Z}_i'\boldsymbol{\Sigma}_{\varepsilon_i}^{-1}\mathbf{u}_i + \mathbf{D}_{\alpha_i}^{-1}\mathbf{d}_{\alpha_i}\right), \\ \overline{\mathbf{D}}_{\alpha_i} = \left(\mathbf{Z}_i'\boldsymbol{\Sigma}_{\varepsilon_i}^{-1}\mathbf{Z}_i + \mathbf{D}_{\alpha_i}^{-1}\right)^{-1}, \end{cases} \tag{A-37}$$

with $\boldsymbol{\Sigma}_{\varepsilon_i} = \sigma^2_{\tilde{e},i} I_T$.

- *Sampling* $\boldsymbol{\sigma}^2_{\tilde{e},i}$, $i = 1, \ldots, N+1$

Recall that $\mathbf{G} = \mathbf{L}_{\mathbf{A}}\mathbf{L}_{\boldsymbol{\Sigma}_{\tilde{e}}}$, where $\mathbf{L}_{\boldsymbol{\Sigma}_{\tilde{e}}} = I_T \otimes \mathtt{diag}\left(\sigma_{\tilde{e},1},\ \cdots,\ \sigma_{\tilde{e},N+1}\right)$. Therefore, we can recast (A-1) as:

$$\mathbf{L_A}^{-1}\left(\widetilde{\mathbf{y}} - \mathbf{W}\boldsymbol{\tau} - \mathbf{X}\boldsymbol{\beta}\right) = \mathbf{L}_{\boldsymbol{\Sigma}_{\tilde{e}}}\tilde{\mathbf{e}} \Longleftrightarrow \tag{A-38}$$

$$\widetilde{\widetilde{\mathbf{y}}} = \tilde{\tilde{\mathbf{e}}} \quad \tilde{\tilde{\mathbf{e}}} \sim \mathcal{N}\left(\mathbf{0}_{(N+1)T\times 1},\ \boldsymbol{\Sigma}_{\tilde{\mathbf{e}}}\right), \tag{A-39}$$

where $\boldsymbol{\Sigma}_{\tilde{\mathbf{e}}} = I_T \otimes \mathtt{diag}\left(\sigma^2_{\tilde{e},1},\ \cdots,\ \sigma^2_{\tilde{e},N+1}\right)$ and $\sigma^2_{\tilde{e},N+1} = \sigma^2_v$.

We assume independent inverse-gamma priors:

$$\sigma^2_{\tilde{e},i} \sim \mathcal{IG}\left(\upsilon_{\tilde{e},i}, S_{\tilde{e},i}\right), \qquad i = 1, \ldots, N+1, \tag{A-40}$$

with hyperparameters calibrated as:

$$\upsilon_{\tilde{e},i} = \frac{T}{10}, \qquad S_{\tilde{e},i} = 1^2\left(\upsilon_{\tilde{e},i} - 1\right), \qquad i = 1, \ldots, N+1. \tag{A-41}$$

Conditional on $(\boldsymbol{\tau}, \boldsymbol{\beta}, A, \boldsymbol{\Sigma}_{\tilde{e},-i})$, the likelihood contribution of $\sigma^2_{\tilde{e},i}$ is obtained from the i-th component of $\tilde{\tilde{\mathbf{e}}}$. Let $\tilde{\tilde{e}}_{t,i}$ denote the i-th element of $\tilde{\tilde{\mathbf{e}}}_t$.

Combining likelihood and prior yields the full conditional posterior:

$$\sigma^2_{\tilde{e},i} \mid \widetilde{\mathbf{y}},\ \boldsymbol{\tau},\ \boldsymbol{\theta}_{-\sigma^2_{\tilde{e},i}} \sim \mathcal{IG}\left(\overline{\upsilon}_{\tilde{e},i},\ \overline{S}_{\tilde{e},i}\right), \text{ where } \begin{cases} \overline{\upsilon}_{\tilde{e},i} = \frac{T}{2} + \upsilon_{\tilde{e},i}, \\ \overline{S}_{\tilde{e},i} = \frac{1}{2}\sum_{t=1}^{T} \tilde{e}_{t,i}{}^2 + S_{\tilde{e},i}, \qquad i = 1, \ldots, N+1. \end{cases} \tag{A-42}$$

- *Sampling* $\boldsymbol{\sigma}^2_{\xi^*,k}$, $k \in \{\pi^*,\ r^*\}$

Recall from (A-2) that the trend-specific disturbances enter through:

$$\mathbf{L}_{\boldsymbol{\tau}}\boldsymbol{\tau} = \boldsymbol{\tau}_0 + \mathbf{L}_{\boldsymbol{\lambda}}\tilde{\mathbf{e}} + \mathbf{L}_{\boldsymbol{\Sigma}_{\tilde{\xi}}}\widetilde{\boldsymbol{\xi}}^*, \tag{A-43}$$

where $\widetilde{\boldsymbol{\xi}}^* \sim \mathcal{N}(\mathbf{0}, I_{2T})$ and $\mathbf{L}_{\boldsymbol{\Sigma}_{\tilde{\xi}}} = I_T \otimes \boldsymbol{\Sigma}^{1/2}_{\xi^*}$ with $\boldsymbol{\Sigma}_{\xi^*} = \texttt{diag}(\sigma^2_{\xi^*,\pi^*}, \sigma^2_{\xi^*,r^*})$.

Conditional on all other parameters and states, define:

$$\mathbf{r}_{\xi} \equiv \mathbf{L}_{\boldsymbol{\tau}}\boldsymbol{\tau} - \boldsymbol{\tau}_0 - \mathbf{L}_{\boldsymbol{\lambda}}\tilde{\mathbf{e}}. \tag{A-44}$$

Then:

$$\mathbf{r}_{\xi} = \mathbf{L}_{\boldsymbol{\Sigma}_{\tilde{\xi}}}\widetilde{\boldsymbol{\xi}}^*, \qquad \mathbf{r}_{\xi} \sim \mathcal{N}\left(\mathbf{0},\ \mathbf{L}_{\boldsymbol{\Sigma}_{\tilde{\xi}}}\mathbf{L}'_{\boldsymbol{\Sigma}_{\tilde{\xi}}}\right). \tag{A-45}$$

Let $r_{\xi,k,t}$ denote the element of the vector $\mathbf{r}_{\xi,t}$ associated with $k \in \{\pi^*,\ r^*\}$, for $t = 1, \ldots, T$. Assume independent inverse-gamma priors:

$$\sigma^2_{\xi^*,k} \sim \mathcal{IG}\left(\upsilon_{\xi^*,k}, S_{\xi^*,k}\right), \qquad k \in \{\pi^*,\ r^*\}, \tag{A-46}$$

with hyperparameters calibrated as:

$$\upsilon_{\xi^*,k} = \frac{T}{10}, \qquad S_{\xi^*,k} = 0.1^2\left(\upsilon_{\xi^*,k} - 1\right), \qquad k \in \{\pi^*,\ r^*\}. \tag{A-47}$$

Combining likelihood and prior yields the full conditional posterior:

$$\sigma^2_{\xi^*,k} \mid \widetilde{\mathbf{y}},\ \boldsymbol{\tau},\ \boldsymbol{\theta}_{-\sigma^2_{\xi^*,k}} \sim \mathcal{IG}\left(\overline{\upsilon}_{\xi^*,k},\ \overline{S}_{\xi^*,k}\right), \text{ where } \begin{cases} \overline{\upsilon}_{\xi^*,k} = \frac{T}{2} + \upsilon_{\xi^*,k}, \\ \overline{S}_{\xi^*,k} = \frac{1}{2}\sum_{t=1}^{T} r_{\xi,k,t}{}^2 + S_{\xi^*,k}, \qquad k \in \{\pi^*,\ r^*\}. \end{cases} \tag{A-48}$$

- *Sampling* $\boldsymbol{\lambda}$

Note that we can re-express the state equation in (A-2) as:

$$\mathbf{L}_{\boldsymbol{\tau}}\boldsymbol{\tau} = \boldsymbol{\tau}_0 + \mathbf{L}_e\boldsymbol{\lambda} + \mathbf{v}, \tag{A-49}$$

where $\mathbf{v} = \mathbf{L}_{\boldsymbol{\Sigma}_{\tilde{\xi}}}\widetilde{\boldsymbol{\xi}}^*$ and hence $\mathbf{v} \sim \mathcal{N}\left(\mathbf{0},\ \mathbf{L}_{\boldsymbol{\Sigma}_{\tilde{\xi}}}\mathbf{L}'_{\boldsymbol{\Sigma}_{\tilde{\xi}}}\right)$.

The matrix $\mathbf{L}_e$ is constructed from the monetary policy shock sequence $\{e_t^{MP}\}_{t=1}^T$ and is given by:

$$\mathbf{L}_e = \begin{bmatrix} e_1^{MP} & 0 \\ 0 & e_1^{MP} \\ e_2^{MP} & 0 \\ 0 & e_2^{MP} \\ \vdots & \vdots \\ e_T^{MP} & 0 \\ 0 & e_T^{MP} \end{bmatrix} = I_2 \otimes \begin{bmatrix} e_1^{MP} \\ e_2^{MP} \\ \vdots \\ e_T^{MP} \end{bmatrix}. \tag{A-50}$$

Since – when sampling $\boldsymbol{\lambda}$ – all parameters and states in (A-1) are given, we can back out the structural shocks $\tilde{\mathbf{e}}$ by simply computing:

$$\tilde{\mathbf{e}} = \left(\mathbf{L}_{\mathbf{A}}\mathbf{L}_{\boldsymbol{\Sigma}_{\tilde{e}}}\right)^{-1}\left(\widetilde{\mathbf{y}} - \mathbf{W}\boldsymbol{\tau} - \mathbf{X}\boldsymbol{\beta}\right). \tag{A-51}$$

Hence, the monetary policy shock sequence $\{e_t^{MP}\}_{t=1}^T$ is directly available from the corresponding component of $\tilde{\mathbf{e}}$.

Conditional on all other parameters, define:

$$\mathbf{y}_\lambda \equiv \mathbf{L}_{\boldsymbol{\tau}}\boldsymbol{\tau} - \boldsymbol{\tau}_0, \tag{A-52}$$

so that (A-49) becomes:

$$\mathbf{y}_\lambda = \mathbf{L}_e\boldsymbol{\lambda} + \mathbf{v}, \qquad \mathbf{v} \sim \mathcal{N}\left(\mathbf{0}, \boldsymbol{\Sigma}_v\right), \tag{A-53}$$

where $\boldsymbol{\Sigma}_v = \mathbf{L}_{\boldsymbol{\Sigma}_{\tilde{\xi}}}\mathbf{L}'_{\boldsymbol{\Sigma}_{\tilde{\xi}}}$.

We assume a Gaussian prior:

$$\boldsymbol{\lambda} \sim \mathcal{N}\left(\mathbf{0}, \boldsymbol{\Sigma}_\lambda\right), \tag{A-54}$$

where $\boldsymbol{\Sigma}_\lambda = I_2$. Combining likelihood and prior yields a Gaussian full conditional posterior:

$$\boldsymbol{\lambda} \mid \widetilde{\mathbf{y}},\ \boldsymbol{\tau},\ \boldsymbol{\theta}_{-\lambda} \sim \mathcal{N}\big(\overline{\mathbf{d}}_\lambda,\ \overline{\mathbf{D}}_\lambda\big)\,,\ \text{where}\ \begin{cases} \overline{\mathbf{d}}_\lambda = \overline{\mathbf{D}}_\lambda \mathbf{L}_e' \boldsymbol{\Sigma}_v^{-1} \mathbf{y}_\lambda, \\ \overline{\mathbf{D}}_\lambda = \left(\mathbf{L}_e' \boldsymbol{\Sigma}_v^{-1} \mathbf{L}_e + \boldsymbol{\Sigma}_{\boldsymbol{\lambda}}^{-1}\right)^{-1}. \end{cases} \tag{A-55}$$